Kallikrein 13: a new player in coronaviral infections.

Aleksandra Milewska[1,2], Katherine Falkowski[2], Magdalena Kalinska[3], Ewa Bielecka[3], Antonina Naskalska[1], Pawel Mak[4], Adam Lesner[5], Marek Ochman[6], Maciej Urlik[6], Jan Potempa[2,7], Tomasz Kantyka[3,8], Krzysztof Pyrc[1,*]

[1] Virogenetics Laboratory of Virology, Malopolska Centre of Biotechnology, Jagiellonian University, Gronostajowa 7a, 30-387 Krakow, Poland.
[2] Microbiology Department, Faculty of Biochemistry, Biophysics and Biotechnology, Jagiellonian University, Gronostajowa 7, 30-387 Krakow, Poland.
[3] Laboratory of Proteolysis and Post-translational Modification of Proteins, Malopolska Centre of Biotechnology, Jagiellonian University, Gronostajowa 7a, 30-387 Krakow, Poland.
[4] Department of Analytical Biochemistry, Faculty of Biochemistry, Biophysics and Biotechnology, Jagiellonian University, Gronostajowa 7 St., 30-387, Krakow, Poland.
[5] University of Gdansk, Faculty of Chemistry, Wita Stwosza 63, 80-308 Gdansk, Poland.
[6] Department of Cardiac, Vascular and Endovascular Surgery and Transplantology, Medical University of Silesia in Katowice, Silesian Centre for Heart Diseases, Zabrze, Poland.
[7] Centre for Oral Health and Systemic Diseases, University of Louisville School of Dentistry, Louisville, KY 40202, USA.
[8] Broegelmann Research Laboratory, Department of Clinical Science, University of Bergen, 5020 Bergen, Norway

* Correspondence should be addressed to **Krzysztof Pyrc (**k.a.pyrc@uj.edu.pl), Virogenetics Laboratory of Virology, Malopolska Centre of Biotechnology, Jagiellonian University, Gronostajowa 7, 30-387 Krakow, Poland; Phone number: +48 12 664 61 21; www: http://virogenetics.info/.

ABSTRACT

Human coronavirus HKU1 (HCoV-HKU1) is associated with respiratory disease and is prevalent worldwide, but *in vitro* model for virus replication is lacking. Interaction between the coronaviral spike (S) protein and its receptor is the major determinant of virus tissue and host specificity, but virus entry is a complex process requiring a concerted action of multiple cellular elements. Here, we show that KLK13 is required for the infection of the human respiratory epithelium and is sufficient to mediate the entry of HCoV-HKU1 to non-permissive RD cells. We also demonstrated HCoV-HKU1 S protein cleavage by KLK13 in the S1/S2 region, proving that KLK13 is the priming enzyme for this virus. Summarizing, we show for the first time that protease distribution and specificity predetermines the tissue and cell specificity of the virus and may also regulate interspecies transmission. It is also of importance that presented data may be relevant for the emerging coronaviruses, including SARS-CoV-2 and may help to understand the differences in their zoonotic potential.

INTRODUCTION

Coronaviruses are the largest group within the order *Nidovirales*. Mainly, they cause respiratory and enteric diseases in humans and animals, but some can cause more serious conditions such as hepatitis, peritonitis, or neurological disease. Seven coronaviruses infect humans, four of which (human coronavirus [HCoV]-229E, HCoV-NL63, HCoV-OC43, and HCoV-HKU1) cause relatively mild upper and lower respiratory tract disease and two (SARS-CoV and MERS-CoV) are associated with severe, life-threatening respiratory infections and multiorgan failure (*1-6*). Furthermore, in December 2019 a novel coronavirus SARS-CoV-2 emerged in Hubei province, China, causing pneumonia. To date, almost 90,000 cases were identified and 3,000 patients died worldwide.

Coronaviral infection is initiated by interaction between the trimeric spike (S) protein and its receptor, which is expressed on the surface of the susceptible cell. A number of adhesion and entry receptors have been described for coronaviruses. For example, HCoV-229E (similar to many other alphacoronaviruses) utilizes aminopeptidase N (APN) as the primary entry port (*7*). Surprisingly, its cousin HCoV-NL63 shares receptor specificity with the evolutionarily distant SARS-CoV and SARS-CoV-2: all hijack angiotensin-converting enzyme 2 (ACE2) (*8-11*). HCoV-NL63 was also shown to use heparan sulfate as a primary attachment site (*12-14*). A very different receptor is recognized by MERS-CoV, which binds to dipeptidyl-peptidase 4 (DPP4) (*9, 15, 16*). Another betacoronavirus, HCoV-OC43, binds to N-acetyl-9-O-acetylneuraminic acid (*17, 18*). HCoV-HKU1 remains the great unknown because its cellular receptor has not been identified and all efforts to culture the virus *in vitro* have failed.

HCoV-HKU1 was identified in Hong Kong in 2004. The virus was present in a sample obtained from an elderly patient with severe pneumonia (*19*). Epidemiological studies show a high prevalence of the pathogen in humans; this is because the majority of children seroconvert before the age of 6 years (*20, 21*). While it is not possible to culture HCoV-HKU1 *in vitro*, we

and others reported that *ex vivo* fully differentiated human airway epithelium (HAE) and human alveolar type II cells support the infection (*22*-*25*). A thorough study by Huang X *et al*. demonstrated that HCoV-HKU1 binds to target cells *via O*-acetylated sialic acids on the cell surface; however, this interaction is not sufficient for the infection. The study also showed that the hemagglutinin-esterase (HE) protein of HCoV-HKU1 exhibits sialate-*O*-acetylesterase activity and may act as a receptor-destroying enzyme, thereby facilitating the release of viral progeny (*26*). Bakkers *et al*. proposed that, in order to adapt to the sialoglycome of the human respiratory tract over the evolutionary timescale, HCoV-HKU1 lost the ability to bind to attachment receptors *via* the HE protein (*27*). Recently, Hulswit *et al*. mapped the virus binding site to *O*-acetylated sialic acids, demonstrating that the S1 domain A is responsible for binding to the attachment receptor (*28*).

The S protein is the main player during coronavirus entry, and its characteristics determine the host range. Coronaviral S proteins are class I fusion proteins comprising a large N-terminal ectodomain, a hydrophobic trans-membrane region, and a small C-terminal endodomain. The ectodomain is highly glycosylated and is composed of S1 and S2 domains. The globular S1 domain is highly variable and carries the receptor-binding site, whereas the more conserved rod-like S2 domain undergoes structural rearrangement during entry, which brings the cellular and viral membranes into close proximity. Such a structural switch may be triggered by different stimuli, including receptor binding, proteolytic cleavage of the S protein, and/or a reduction in pH. Because different species require different stimuli, coronaviruses enter cells at different subcellular sites. Some coronaviruses fuse at the plasma membrane, whereas others are believed to enter the cell through receptor-mediated endocytosis, followed by fusion deep within the endosomal compartments (*29*-*35*). Furthermore, recent reports show that the

entry portal may vary depending on tissue/cell characteristics. These differences may affect the host range, pathogenicity, and cell/tissue specificity (*1*).

Host proteases prime coronaviral S proteins. For example, trypsin-mediated cleavage in the small intestine is required for entry of porcine epidemic diarrhea virus (*36*), while a number of coronaviruses from different genera (including HCoV-OC43, HCoV-HKU1, murine hepatitis virus [MHV], MERS-CoV, and infectious bronchitis virus [IBV]) possess a furin cleavage site (*37-41*). Kam *et al.* showed that SARS-CoV S protein can be cleaved by plasmin; however, there is almost no biological evidence for its role *in vivo* (*42*). Cathepsins may also act as S protein-activating enzymes. Indeed, cathepsin L processes the S proteins of SARS-CoV, MERS-CoV, HCoV-229E, and MHV-2 (*43-46*). However, recent reports show that, *in vivo*, respiratory coronaviruses may be activated by the TMPRSS2 protease, which enables endocytosis-independent internalization, thereby re-shaping the entry process (*45, 47-50*). While laboratory strains require priming by cathepsins, S proteins of clinical isolates (e.g., HCoV-229E and HCoV-OC43) undergo TMPRSS2-mediated cleavage at the cell surface, which enables them to fuse with the cell membrane on the cell surface (*51*). A recent study by Shirato *et al*. demonstrates that coronaviruses may lose their ability to infect naturally permissive HAE cultures during cell culture adaptation because the S gene evolves and adjusts to the proteolytic landscape of the immortalized cells (*51*).

Here, we identified a protease belonging to the tissue kallikrein (KLK) family as a new player essential for HCoV-HKU1 entry to the target cell. The KLK family comprises 15 closely related serine proteases with trypsin- or chymotrypsin-like specificity. The expression of these enzymes is tightly regulated, and each tissue has its own unique KLK expression profile. These enzymes play a role in a diverse range of processes during embryonic development to adulthood (*52-56*), and some have been linked to human cancers (*57-60*). The function of some KLKs remains to be elucidated, but obtained results suggest that protease distribution may be an

121 important factor pre-determining the cell and tissue specificity of the virus, but also regulating
122 the interspecies transfers.

123 Further, the data presented herein bring us a step closer to developing a convenient
124 *in vitro* culture model and possibly identifying the cellular receptor for this virus. It is also of
125 importance that presented data may be relevant for the emerging coronaviruses and may help
126 to understand the differences in their zoonotic potential.

RESULTS

Several KLKs are upregulated after infection of HAE with HCoV-HKU1

First, we asked whether HCoV-HKU1 infection modulates the expression of human KLKs. HAE cultures were infected with HCoV-HKU1 or mock-inoculated. At 120 h post-inoculation (p.i.), cells were collected and the expression of mRNAs encoding KLKs was analyzed. We detected the expression of KLK7, KLK8, KLK10, KLK11, and KLK13 in non-infected fully differentiated cultures. However, the pattern in HCoV-HKU1-infected cells was different: we detected an upregulation of KLK7, KLK8, KLK10, KLK11 and KLK13. Further, KLK1, KLK5, KLK6, KLK9, KLK12 and KLK14 were expressed in the infected cells. KLK2, KLK3, and KLK15 were not expressed (**Fig. 1**).

KLK13 is essential for HCoV-HKU1 infection

S protein priming is a prerequisite for coronavirus entry; therefore, we tested whether KLKs take part in this process by culturing cells in the presence/absence of KLK inhibitors (**Table 1**) (*61*). For this, HAE cultures were pre-incubated with each inhibitor (10 μM) or with vehicle control (DMSO) and mock-inoculated or inoculated with the virus (10^6 RNA copies per ml) in the presence of the inhibitor. Apical washes were collected each day for analysis of virus replication. Subsequently, viral RNA was isolated and reverse transcribed (RT), and the HCoV-HKU1 yield was determined by quantitative real-time PCR (qPCR). The results showed that HCoV-HKU1 replication was inhibited in the presence of a KLK13 inhibitor; this was not the case for cells treated with DMSO or with inhibitors specific for KLK7 or KLK8 (**Fig. 2A**).

Next, we analyzed HCoV-HKU1 replication in the presence of a family-specific KLK inhibitor SPINK6 at a concentration of 10 μg/ml (*62*, *63*) or 100 μM camostat (a broad inhibitor of serine proteases, also a potent inhibitor of KLK13) (*34*, *64*). We noted inhibition of

HCoV-HKU1 replication in the presence of both inhibitors (**Fig. 2B**). All inhibitors were used at non-toxic concentrations (**Fig. 2C**).

The experiments conducted so far suggested that KLK13 is required for virus infection. However, one may question the specificity of the KLK13 protease inhibitors. To ensure that KLK13 is indeed the priming enzyme during HCoV-HKU1 infection, we developed HAE cultures by transforming cells with lentiviral vectors encoding shRNAs targeting KLK13 mRNA. We then confirmed that the expression of the protease was silenced (HAE_shKLK13). Non-modified HAE cultures (HAE_ctrl), cultures modified using a lentiviral vector to express the GFP protein (HAE_GFP), and HAE cultures transduced with an empty lentiviral vector (HAE_vector) were used as controls. Following transduction and differentiation, expression of KLK13 mRNA in HAE_shKLK13 was almost undetectable, in contrast to the control cultures (**Fig. 3A**). Importantly, HAE_shKLK13 cells continued to differentiate and formed pseudostratified cultures (**Fig. 3B**). Next, we infected HAE_ctrl, HAE_GFP, HAE_vector, and HAE_shKLK13 with HCoV-HKU1 (10^6 RNA copies per ml) and incubated them for 2 h at 32°C with the viral stock solution. Cultures were maintained at 32°C for 5 days at an air-liquid interface. Apical washes were collected, and virus yield was determined by RT-qPCR. We found that, in contrast to that in control cultures, replication of virus in HAE_shKLK13 was abolished (**Fig. 3C**). Overall, these data suggest that silencing the *KLK13* gene in HAE inhibits virus infection, indicating that KLK13 is necessary for HCoV-HKU1 infection.

KLK13 enables entry of HCoV-HKU1 pseudoviruses

We determined that KLK13 is essential for efficient HCoV-HKU1 infection in HAE cultures and we started to wonder whether this enzyme may be a determinant of the cell and tissue specificity of the virus. Previous studies showed that RD cells support virus attachment *via* sialic acids, but this does not allow for the virus entry (*26*). To test whether cell surface

proteases my render RD cells permissive, we generated RD cells expressing human KLK13 or TMPRSS2 proteases. RD cells were transduced with lentiviral vectors harboring the KLK13 gene (RD_KLK13), control vector (RD_ctrl), or TMPRSS2 (RD_TMPRSS2). Due to the lack of KLK13 specific antibodies, we verified its presence based on RT-PCR (**Fig. 4A**). The presence of TMPRSS2 in RD_TMPRSS2 cells was confirmed using Western blot. The TMPRSS2 band in RD cells was observed at 25 kDa, which corresponds to one of the naturally occurring splicing variants (**Fig. 4B**). Subsequently, we transduced RD_ctrl, RD_KLK13 and RD_TMPRSS2 cells with HIV particles pseudotyped with HCoV-HKU1 S glycoprotein (S-HKU1), control VSV G protein (VSV-G) or lacking the fusion protein (ΔEnv). After 3 day culture at 37°C, pseudovirus entry was quantified by measurement of the luciferase activity. As shown in **Fig. 4C**, all cultures were effectively transduced with control VSV-G vectors, while only RD_KLK13 cells were permissive to S-HKU1 pseudoviruses. This clearly showed that KLK13, and not TMPRSS2 is involved in HCoV-HKU1 entry. Furthermore, S-HKU1,d VSV-G and ΔEnv pseudoviruses were overlaid onto fully differentiated HAE cultures in the presence of KLK13 inhibitor (10 μM) or DMSO. After 3 day culture at 37°C pseudovirus entry was quantified by measurement of the luciferase activity. Despite low transduction efficiency in HAE, we observed an increase in luciferase activity in cultures treated with S-HKU1 pseudoviruses, compared to ΔEnv, which was completely abolished in the presence of KLK13 inhibitor (**Fig 4D**). Overall, these data demonstrated that KLK13 activity drives HCoV-HKU1 entry into cells.

KLK13 enables the replication of HCoV-HKU1 in RD cells

Obtained results showed that KLK13 expression on RD cells was sufficient for HCoV-HKU1 pseudovirus entry. Here, we aimed to test whether KLK13 presence renders RD cells permissive for HCoV-HKU1 infection. For this, we infected RD_ctrl and RD_KLK13 cells

with HCoV-HKU1 (10^8 RNA copies per ml) and incubated the culture for 7 days at 32°C in the presence or absence of a KLK13 inhibitor (10 μM) or DMSO. Next, cellular RNA was isolated and the presence of HCoV-HKU1 N subgenomic mRNA (N sg mRNA), which is considered to be a hallmark of coronaviral infection, was assessed (*14*). sg mRNA appeared in RD_KLK13 cells, while no signal was detected in cultures supplemented with the KLK13 inhibitor nor in RD_ctrl cells (**Fig. 5A**).

To further confirm the role of KLK13 during HCoV-HKU1 infection RD cells were supplemented with purified human KLK13 or KLK14 (*61*). The latter was used as a negative control. Virus stock was incubated for 2 h at 32°C with 200 nM KLK13, KLK14, or trypsin or control (PBS). Next, RD cells were incubated for 7 days at 32°C with the virus (diluted 10-fold in DMEM) or mock samples (in DMEM), after which cellular RNA was isolated and HCoV-HKU1 infection was analyzed by means of N sg mRNA detection. Again, we found that N sg mRNA was produced only in the presence of KLK13 (**Fig. 5B**). Further, we passaged HCoV-HKU1 twice in RD cells. Briefly, 1 ml of cell culture supernatant from the first experiment was transferred to fresh RD cells and fresh enzymes were added (final concentration 200 nM). Cultures were then incubated at 32°C for 7 days. Cellular RNA was isolated and HCoV-HKU1 infection was monitored by detecting N sg mRNA. The infection occurred only in the presence of KLK13 (**Fig. 5B**). However, we observed no cytopathic effects (CPEs), and replication levels were very low (no significant increase over control levels on RT-qPCR; data not shown). To further test the effect of KLK13 on replication of HCoV-HKU1 in RD cells, the virus stock was incubated with purified KLK13 (200 nM) and incubated in the presence or absence of a KLK13 inhibitor (10 μM) or DMSO. After 2 h at 32°C pre-treated virus stock was diluted in media as described above and overlaid on RD cells. After 7 days at 32°C we evaluated the presence of the HCoV-HKU1 N sg mRNA. The virus replicated only after treatment with KLK13, and supplementation with the inhibitor blocked this effect infection (**Fig. 5C**).

226

227 **KLK13 primes the HCoV-HKU1 S protein**

228 Expression of KLK13 by cells previously resistant to HCoV-HKU1 renders them
229 susceptible; therefore, we asked whether this is due to proteolytic activation of the S protein.
230 We tested this using the CleavEx method, in which a peptide of interest is exposed in the
231 N-terminal region of the proteolytically-resistant HmuY carrier protein. Briefly, two-hybrid
232 His-tagged CleavEx proteins were prepared, both harboring 8-amino acid peptide sequences of
233 the HCoV-HKU1 S protein. The first peptide contained the S1/S2 cleavage site (amino acids
234 757–764), which in some coronaviruses is activated during protein biosynthesis, during virus
235 exocytosis, or after receptor engagement. The second harbored the S2/S2' cleavage site (amino
236 acids 901–908), which is an additional region prone to proteolytic cleavage (*25*, *38*). Proteins
237 were purified and further incubated for 3 h at 37°C with increasing concentrations of purified
238 KLK13. Subsequently, proteins were resolved by SDS-PAGE and detected by western blotting
239 with antibodies specific for His-tagged proteins. The analysis showed that, in the presence of
240 500 nM KLK13, the CleavEx protein harboring the S1/S2 cleavage site was degraded; however,
241 the CleavEx protein harboring the S2/S2' site remained intact. Because KLKs are produced as
242 pro-forms that undergo self-activation, an additional band of His-tagged purified pro-KLK13
243 (HisTag-pro-KLK13) was observed after treatment with 500 nM KLK13 (**Fig. 6A**). The product
244 of the S1/S2 cleavage was further sequenced by N-terminal Edman degradation showing the
245 following sequence: R↓SISA, which corresponds to the S1/S2 site. This result shows clearly
246 that the S1/S2 region of the HCoV-HKU1 S protein is prone to KLK13-mediated cleavage.

247 Furthermore, we aimed to confirm the cleavage using a full-length Spike protein of
248 HCoV-HKU1 (HKU1-S). For this, we expressed the HKU1-S in 293T cells, purified the protein
249 using 6 × His tag, and incubated for 3 h at 37°C with increasing concentrations of purified
250 KLK13. Subsequently, HKU-S or mock proteins were resolved by SDS-PAGE and detected by

251 western blotting with antibodies specific to the tag. The analysis showed that in the presence of
252 1 μM KLK13 the HKU1-S was degraded (**Figure 6B**). The S protein was observed at
253 ~150 kDa, which is consistent with the migration speed reported for these highly glycosylated
254 proteins (*1*).
255

DISCUSSION

Receptor recognition is the first, essential step of the virus infection process. The coronaviral S protein mediates virus entry into host cells by binding to a specific receptor. A combination of stimuli, e.g., receptor binding, proteolytic cleavage, and exposure to low pH results in rearrangement of the S protein and, consequently, to membrane fusion and virus entry (*1*). Although the structure of both the HCoV-HKU1 S ectodomain and the receptor-binding domain has been resolved, the receptor determinant remains unknown (*28, 38, 65*). In a previous study, we showed that HCoV-HKU1 utilizes *O*-acetylated sialic acids on host cells as an attachment receptor (*26*). Here, we present data demonstrating that the protease KLK13 is required for HCoV-HKU1 infection of the respiratory epithelium.

Human KLKs take part in multiple physiological processes, including skin desquamation, tooth enamel formation, kidney and brain function, and synaptic neural plasticity (*66-75*). Also, recent studies demonstrate a role for some KLKs during viral infections. For instance, KLK8 plays a role in the proteolytic activation of the human papillomavirus capsid protein, thereby mediating virus entry into host cells (*76*). Also, KLK5 and KLK12 are secreted into the respiratory tract, where they support replication of the influenza A virus by cleaving the hemagglutinin protein (*77, 78*); however, these proteins belong to a large pool of cell surface proteases, the orchestrated action of which promotes virus replication.

Here, we found that the yield of HCoV-HKU1 from HAE fell in the presence of SPINK6 (inhibitor of KLK13) (*62, 63*) and camostat (a broad range inhibitor of serine proteases). However, the first compound also inhibits other KLKs (*63*), while the second block the activity of a wide range of serine proteases and was used previously to demonstrate the role of TMPRSS2/4 proteases during viral infection (*34, 45, 51, 64, 79, 80*). The relatively low inhibition of HCoV-HKU1 replication in the presence of SPINK6 possibly results from non-optimal compound concentration at the HAE cultures, and cytotoxicity at higher

concentrations(*63*). Broad spectrum protease inhibitors are now used widely for virus research, although their non-specific activity makes the results equivocal. For example, Matsuyama *et al*. showed recently that the furin inhibitor dec-RVKR-CMK interferes with the activity of several proteases, and that its previously described inhibitory activity during MERS-CoV infection is not specific to furin; instead, its activity is due to non-specific inhibition of cathepsin L and TMPRSS2 (*81*). We tried to use specific KLK inhibitors developed in our laboratory (*61*). Considering the small arsenal of tools available to researchers studying KLKs, only three compounds were readily available. Treating HAE cultures with these inhibitors revealed that only compounds designed to inhibit KLK13 hampered HCoV-HKU1 replication. However, the great similarity between different KLKs makes one doubt the specificity of these inhibitors, despite their performance in biochemical assays. Therefore, we decided to silence KLK13 in HAE cultures. This abolished virus replication *ex vivo*, thereby confirming the importance of KLK13 during infection. KLK13 is thought to be secreted and membrane-bound(*82, 83*).

This study showed that HCoV-HKU1 infection in HAE modulates the expression of different KLKs, including KLK13. In our study, KLKs expression was tested using semi-quantitative PCR, and for that reason, we were unable to show the level of KLKs modulation after HCoV-HKU1. However, the pattern of virus-induced expression of several KLKs could be observed. KLK mechanism of activation is a complex process and until now it has only been proven that most KLK genes are regulated by steroids and other hormones (*84*). It is also important to remember, that KLK expression is regulated in a similar manner, and the induction of a single gene usually results in overexpression of the whole cluster (*85, 86*). While one may assume that the virus stimulates KLK13 production to promote the infection, this up-regulation is likely a natural response of the damaged tissue, as KLKs were previously reported to take part also in tissue regeneration (*87-89*). Further, increased expression of KLKs may be the

response to the inflammatory process, as Seliga *et al* demonstrated that KLK-kinin system is a potent modulator of innate immune responses (*90*).

The experiments performed herein show the importance of KLK13 for virus entry into susceptible cells; therefore, we speculated that scattered distribution of different KLKs in different tissues may be one of the determinants of the HCoV-HKU1 tropism (*53*, *91*). We tested the purified enzyme expressed in the eukaryotic cells; however, we also developed a cell line constitutively expressing the enzyme. As an *in vitro* model for our studies, we used RD cells previously reported to carry attachment receptors for the virus (*26*). Here, using pseudoviruses decorated with S-HKU1 proteins we showed that KLK13 presence on RD cells is sufficient for virus entry and renders these cells permissive. Our experiments also showed that in contrast to previous reports, TMPRSS2 is not involved in this process(*51*). Furthermore, we observed that RD cells supported the replication of the virus in the presence of KLK13 and that this effect was reversed in the presence of the specific KLK13 inhibitor. We were, however, not able to culture the virus to high yields. HCoV-HKU1 replication in KLK13-expressing RD cells remained inefficient and RTqPCR assessment did not reveal significant increases in the amounts of viral RNA. For that reason, we are only able to detect viral sg mRNAs, which are considered to be the hallmark of coronaviral replication.We believe that this may be due to non-optimal infection conditions, which may include inappropriate KLK13 concentrations or low density of the entry receptor. Also, it is possible that RD cells may not support efficient replication of the virus due to factors unrelated to the entry process. Nonetheless, our results show that the HCoV-HKU1 entry receptor is present on RD cells, and we were able to trigger virus entry and replication; these findings warrant further exploration.

Most coronaviral S proteins are processed into S1 and S2 subunits by host proteases, which allows conformational changes in the S protein and leads to fusion of the viral and cellular membranes (*1*, *92*). As shown in the recent work by Kirchdoerfer *et al*., the

HCoV-HKU1 S protein has two regions that are prone to proteolytic activation: the S1/S2 furin cleavage site and a secondary cleavage site termed S2', which is adjacent to a potential fusion peptide (*38*). While the S1/S2 site is believed to be processed by furin during protein biosynthesis, the S2/S2' site is expected to be cleaved during virus entry. As we already knew that KLK13 is sufficient for HCoV-HKU1 infection of naturally non-permissive RD cells, we aimed to investigate whether this was the direct result of KLK13-mediated proteolytic cleavage of the S protein. For this, we employed the CleavEx method, in which peptide of interest is coupled to the carrier HmuY protein and then undergoes proteolytic cleavage by the enzyme being tested. We found that the S1/S2 site was efficiently cleaved by KLK13, whereas the S2/S2' region remained intact. As CleavEx technique is a convenient surrogate system allowing for precise mapping of the cleavage site, it has some limitations. To ensure the reliability of results, purified full-length HCoV-HKU1 S protein was subjected to the proteolytic cleavage. Also here we observed efficient cleavage of the HCoV-HKU1 S protein by KLK13.

While the results presented here show that KLK13 is able to process the HCoV-HKU1 S protein, one may question whether the cleavage is sufficient for HCoV-HKU1 entry. It was previously presented for MERS-CoV that two consecutive enzymatic scissions are required for activation of the S protein. In this scenario, KLK13 would prime the HCoV-HKU1 S at S1-S2 site, enabling scission at S2-S2' site by the TMPRSS2 or another host protease (*38, 40, 93*). This may be one of the factors limiting the HCoV-HKU1 replication in RD_KLK13 cells, as only minimal replication is observable.

Summarizing, we show that KLK13 is a key determinant of HCoV-HKU1 tropism. This may explain why, since its first identification in 2004, all efforts to culture HCoV-HKU1 in standard cell lines have failed. We believe that this study increases our knowledge of HCoV-HKU1 and may promote the future in-depth investigation of coronaviruses. Considering the increasing number and diversity of coronaviruses, and the proven propensity of coronaviruses

355 to cross the species barrier and cause severe diseases in humans, further research on the role of

356 different proteases in coronaviral infections is necessary.

MATERIALS AND METHODS

Plasmid constructs

KLK13 and TMPRSS2 genes were amplified by PCR using cDNA obtained from HAE cells. Each PCR product was cloned into pWPI plasmid for lentivirus production and sequence verified. pLKO.1-TRC cloning vector was a gift from David Root (Addgene plasmid # 10878)(*94*). Oligonucleotides for the generation of shRNA against KLK13 (3 different shRNAs targeting the exons encoding the active site) were hybridized and cloned into pLKO.1-TRC vector. The full-length HKU1-S gene was amplified by PCR using pCAGGS/HKU1-S plasmid that was a gift from Xingchuan Huang. The PCR product was cloned into pSecTag2 cloning vector and sequence verified. Primer sequences are provided in **Table 2**.

Cell culture

RD (*Homo sapiens* muscle rhabdomyosarcoma; ATCC: CCL-135) and 293T (*Homo sapiens* kidney epithelial; ATCC: CRL-3216) cells were cultured in Dulbecco's MEM (Thermo Fisher Scientific, Poland) supplemented with 3% fetal bovine serum (heat-inactivated; Thermo Fisher Scientific, Poland) and antibiotics: penicillin (100 U/ml), streptomycin (100 μg/ml), and ciprofloxacin (5 μg/ml). Cells were maintained at 37°C under 5% CO_2.

Human airway epithelium (HAE) cultures

Human epithelial cells were isolated from conductive airways resected from transplant patients. The study was approved by the Bioethical Committee of the Medical University of Silesia in Katowice, Poland (approval no: KNW/0022/KB1/17/10 dated 16.02.2010). Written consent was obtained from all patients. Cells were dislodged by protease treatment, and later mechanically detached from the connective tissue. Resulting primary cells were first cultured in the selective media to proliferate in the presence of the Rho-associated protein kinase

(ROCK) inhibitor (Y-27632, 10 µg/ml, Sigma-Aldrich, Poland) (*95*). Further, cells were trypsinized and transferred onto permeable Transwell insert supports (ϕ = 6.5 mm). Cell differentiation was stimulated by the media additives and removal of media from the apical side after the cells reached confluence. Cells were cultured for 4-6 weeks to form well-differentiated, pseudostratified mucociliary epithelium (*96*). All experiments were performed in accordance with relevant guidelines and regulations.

Cell viability assay

HAE cultures were prepared as described above. Cell viability assay was performed by using the XTT Cell Viability Assay (Biological Industries, Israel), according to the manufacturer's instructions. Briefly, on the day of the assay 100 µl of the 1 × PBS with the 30 µl of the activated XTT solution was added to each well/culture insert. Following 2 h incubation at 37°C, the solution was transferred onto a 96-well plate and the signal was measured at λ = 490 nm using the colorimeter (Spectra MAX 250, Molecular Devices). The obtained results were further normalized to the control sample, where cell viability was set to 100%.

Virus infection

HAE cultures were washed thrice with 100 µl of 1 × PBS, following inoculation with HCoV-HKU1 (strain Caen 1) or mock (cell lysate). After 2 h incubation at 32°C unbound virions were removed by washing with 100 µl of 1 × PBS and HAE cultures were cultured at air-liquid interphase until the end of the experiment. Due to the lack of a permissive cell line it was not possible to titrate the virus stock for infection experiments and therefore the inoculum was quantified using RT-qPCR.

406 RD cells grown in 90% confluency were infected with HCoV-HKU1 (10^8 RNA copies per
407 ml) in Dulbecco's MEM (Thermo Fisher Scientific, Poland) supplemented with 3% fetal bovine
408 serum (heat-inactivated; Thermo Fisher Scientific, Poland) and antibiotics: penicillin
409 (100 U/ml), streptomycin (100 µg/ml). Cells were incubated for seven days at 32°C, washed
410 thrice with 1 × PBS, and collected for RNA isolation in Fenozol reagent (A&A Biotechnology,
411 Poland). All research involving the infectious material was carried out adhering to the biosafety
412 regulations. All research involving genetic modifications was carried out adhering to the
413 national and international regulations.
414
415 **Lentivirus production and transduction**
416 293T cells were seeded on 10 cm^2 dishes, cultured for 24 h at 37°C with 5% CO_2 and
417 transfected with psPAX, pMD2G and third transfer plasmid (pWPI/KLK13, pLKO.1-
418 TRC/shrnaKLK13 or Lego-G2) using polyethyleneimine (Sigma-Aldrich, Poland). psPAX
419 (Addgene plasmid # 12260) and pMD2G (Addgene plasmid # 12259) was a gift from Didier
420 Trono. pLKO.1 - TRC cloning vector was a gift from David Root (Addgene plasmid # 10878)
421 (*94*). Cells were further cultured for 96 h at 37°C with 5% CO_2 and lentiviral particles were
422 collected every 24 h and stored at 4°C. Lentivirus stocks were concentrated 25-fold using
423 centrifugal protein concentrators (Amicon Ultra, 10-kDa cutoff; Merck, Poland) and stored at -
424 80°C.
425 RD cells were seeded in T75 flasks, cultured for 24 h at 37°C with 5% CO_2 and
426 transduced with lentiviral particles harboring KLK13, TMPRSS2 gene or control vector in the
427 presence of polybrene (4 µg/ml; Sigma-Aldrich, Poland). Cells were further cultured for 72 h
428 at 37°C with 5% CO_2 and positively transduced cells were selected using blasticidin (2 µg/ml
429 Sigma-Aldrich, Poland). Primary human epithelial cells seeded on 10 cm^2 dishes were cultured
430 in BEGM medium and transduced with lentiviral particles harboring shRNA against KLK13 (a

set of 3) or GFP gene in the presence of polybrene (5 µg/ml; Sigma-Aldrich, Poland). Cells were further cultured for 72 h at 37°C with 5% CO_2 and positively transduced cells were selected using puromycin (5 µg/ml Sigma-Aldrich, Poland). Selected cells were plated on insert supports and further cultured in ALI in the presence of puromycin (1 µg/ml).

Pseudoviruses

293T cells were seeded on 6-wells plates, cultured for 24 h at 37°C with 5% CO_2 and transfected using polyethyleneimine (Sigma-Aldrich, Poland) with the lentiviral packaging plasmid (psPAX), the VSV-G envelope plasmid (pMD2G) or HCoV-HKU1 S glycoprotein (pCAGGS-HKU1-S) and third plasmid encoding luciferase (pRR Luciferase). pRR Luciferase was a gift from Paul Khavari (Addgene plasmid # 120798) (*97*). Cells were further cultured for 72 h at 37°C with 5% CO_2 and pseudoviruses were collected every 24 h and stored at 4°C.

RD cells were seeded in 48-wells plates, cultured for 24 h at 37°C with 5% CO_2 and transduced with pseudoviruses harboring VSV-G or S-HKU1 proteins or lacking the fusion protein (Δ Env) in the presence of polybrene (4 µg/ml; Sigma-Aldrich, Poland). HAE cultures were washed thrice with 100 µl of 1 × PBS and subsequently inoculated with S-HKU1 or VSV-G pseudoviruses. After 4 h incubation at 37°C unbound virions were removed by washing with 100 µl of 1 × PBS and HAE cultures were cultured at an air-liquid interphase. Cells were further cultured for 72 h at 37°C with 5% CO_2 and lysed in luciferase substrate buffer (Bright-Glo; Promega, Poland). Lysates were transferred onto white 96-wells plates and luciferase levels were measured on a microplate reader Gemini EM (Molecular Devices, UK).

Isolation of nucleic acids and reverse transcription (RT)

Viral DNA/RNA Kit (A&A Biotechnology, Poland) was used for nucleic acid isolation from cell culture supernatants, according to the manufacturer's instructions. Cellular RNA was

isolated using Fenozol reagent (A&A Biotechnology, Poland), followed by DNase I treatment (Thermo Fisher Scientific, Poland). cDNA samples were prepared with a High Capacity cDNA Reverse Transcription Kit (Thermo Fisher Scientific, Poland), according to the manufacturer's instructions.

PCR

Human KLKs mRNA was reverse transcribed and amplified in a reaction mixture containing 1 × Dream *Taq* Green PCR master mix (Thermo Fisher Scientific, Poland) and appropriate primers (**Table 3**; 500 nM each). β-actin was used as a household gene reference. The reaction was carried out according to the scheme: 5 min at 95°C, followed by 35 cycles of 30 s at 95°C, 20 s at 59°C and 20 s at 72°C, followed by 10 min at 72°C.

Quantitative PCR (qPCR)

HCoV-HKU1 RNA yield was assessed using real-time PCR (7500 Fast Real-Time PCR; Life Technologies, Poland). cDNA was amplified in a reaction mixture containing 1 × TaqMan Universal PCR Master Mix (Thermo Fisher Scientific, Poland), in the presence of FAM / TAMRA (6-carboxyfluorescein / 6-carboxytetramethylrhodamine) probe (100 nM; 5' – TTGAAGGCTCAGGAAGGTCTGCTTCTAA– 3') and primers (450 nM each; forward: 5' – CTGGTACGATTTTGCCTCAA – 3' and reverse: 5' -ATTATTGGGTCCACGTGATTG– 3') (*98*). The reaction was carried out according to the scheme: 2 min at 50°C and 10 min at 92°C, followed by 40 cycles of 15 s at 92°C and 1 min at 60°C.

Detection of HCoV-HKU1 N sg mRNA

Total nucleic acids were isolated from virus or mock-infected cells at 7 days p.i. using Fenozol reagent (A&A Biotechnology, Poland), according to the manufacturer's instructions.

Reverse transcription was performed using a high-capacity cDNA reverse transcription kit (Life Technologies, Poland), according to the manufacturer's instructions. Viral cDNA was amplified in a 20 µl reaction mixture containing 1 × Dream *Taq* Green PCR master mix (Thermo Fisher Scientific, Poland), and primers (500 nM each). The following primers were used to amplify HCoV-HKU1 subgenomic mRNA (sg mRNA): common sense primer (leader sequence), 5 – TCTTGTCAGATCTCATTAAATCTAAACT -3'; nucleocapsid antisense for 1st PCR, 5' – AACTCCTTGACCATCTGAAAATTT – 3'; nucleocapsid antisense for nested PCR, 5' – AGGAATAATGTGGGATAGTATTT – 3'. The conditions were as follows: 3 min at 95°C, 35 cycles (30 cycles for nested PCR) of 30 s at 95°C, 30 s at 49°C, and 20 s at 72°C, followed by 5 min at 72°C and 10 min at 4°C. The PCR products were run on 1% agarose gels (1Tris-acetate EDTA [TAE] buffer) and analyzed using molecular imaging software (Thermo Fisher Scientific, Poland).

Detection of TMPRSS2 protease

After blasticidin selection, RD cells expressing TMPRSS2 (RD_TMPRSS2), KLK13 (RD_KLK13) or control cells (RD_ctrl) were scraped and collected by centrifugation. Cells were lysed in RIPA buffer (50 mM Tris, 150 mM NaCl, 1% Nonidet P-40, 0.5% sodium deoxycholate, 0.1% SDS, pH 7.5), boiled for 5 min, cooled on ice, and separated on 10% polyacrylamide gel alongside dual-color Page Ruler Prestained Protein size markers (Thermo Fisher Scientific, Poland). The separated proteins were then transferred onto a Westran S PVDF membrane (GE Healthcare, Poland) by wet blotting (Bio-Rad, Poland) for 1 h, 100 Volts in transfer buffer (25 mM Tris, 192 mM glycine, 20% methanol) at 4°C. The membranes were blocked by overnight incubation at 4°C in TBS-Tween (0.1%) buffer supplemented with 5% skimmed milk (BioShop, Canada). A mouse monoclonal anti-TMPRSS2 antibody (clone P5H9-A3; 1:500 dilution; Sigma-Aldrich, Poland), followed by incubation with a horseradish

peroxidase-labeled anti-mouse IgG (65 ng/ml; Dako, Denmark) diluted in 5% skimmed milk / TBS-Tween (0.1%). The signal was developed using the Pierce ECL Western blotting substrate (Thermo Scientific, Poland) and visualized using the ChemiDoc Imaging System (Bio-Rad, Poland).

Expression and purification of KLK13 and KLK14

The proKLK13 gene was amplified using cDNA obtained from HAE cultures and specific primers. The codon-optimized proKLK14 gene was custom-synthesized (Thermo Scientific, Poland). The products were cloned into the pLEXSY_I-blecherry3 plasmid (Jena Bioscience, Germany) and the resulting constructs were verified by sequencing. All preparations for transfection, selection, and expression of the host *Leishmania tarentolae* strain T7-TR were performed according to the Jena Bioscience protocol for inducible expression of recombinant proteins secreted to medium (LEXSinduce Expression kit, Jena Bioscience, Germany). Expression of proKLK13 and proKLK14 was induced with 15 µg/ml of tetracycline (BioShop, Canada) and carried out for 3 consecutive days. Culture media were collected and precipitated with 80% ammonium sulfate, spun down at 15,000 × g for 30 min at 4°C. Pellets were suspended in 10mM sodium phosphate pH 7.5 and dialyzed overnight at 4°C into 10mM sodium phosphate pH 7.5. The KLKs were isolated *via* the 6 × His tag using nickel resin (GE Healthcare, Poland) according to the manufacturer's protocol. Obtained fractions were analyzed by SDS PAGE in reducing conditions and fractions containing proKLK13 or proKLK14 were concentrated with Vivaspin® 2 (Sartorius, Germany) and further purified using size exclusion chromatography (Superdex s75 pg; GE Healthcare, Poland). Fractions containing proKLK13 or proKLK14 were concentrated and the buffer was changed to 50mM Tris pH 7.5, 150 mM NaCl. After purification and self-activation at 37°C for 24 h, activity of

proteases was assessed by serine protease inhibitor Kazal-type 6 (SPINK6) titration, as described previously (*63*).

Cloning of HmuY-based CleavEx fusion proteins

The fusion constructs were based on positions 26-216 of the *Porphyromonas gingivalis* HmuY protein-encoding gene (accession number ABL74281.1), employed as a carrier protein. The gene was amplified using Phusion DNA polymerase (Thermo Scientific, Poland) and specific primers (forward: 5'– ATATGCGGCCGCAGACGAGCCGAACCAACCCTCCA – 3' and reverse: 5' – ATACTCGAGTTATTTAACGGGGTATGTATAAGCGAAAGTGA – 3') from whole-genomic DNA isolated from *Porphyromonas gingivalis* strain W83. PCR conditions were as follows: 98°C for 30s, followed by denaturation at 98°C for 10s, annealing at 68°C for 40s and extension at 72°C for 30s/kb over 35 cycles with a final extension at 72°C for 7 min. Then, the HmuY gene was further amplified in the three consecutive PCR reactions with primers specific to the 5' HmuY fragment and 3'-specific primer introducing additional nucleotides dependent on the designed sequence (proKLK13 primers, **Table 4**). The reaction was ligated into a modified pETDuet plasmid (potential tryptic cleavage sites were removed from the MCS) using Quick Change mutagenesis using Phusion DNA polymerase (Thermo Scientific, Poland). Alternatively, the designed fusion protein-encoding sequences were produced using Phusion Site-Directed Mutagenesis (Thermo Scientific, Poland), *via* sequence exchange of the previously prepared CleavEx construct (HKU1-S primers, **Table 4**). The final product was transformed into competent *E. coli* T10 cells and further purified and sequenced.

Expression and purification of CleavEx fusion proteins

Protein expression was performed in *E. coli* BL21 and was induced by the addition of 0.5 mM IPTG to the bacterial culture (OD_{600} 0.5-0.6), followed by shaking for 3h at 37°C.

555 Then, the bacteria were spun down and the pellet was suspended in buffer A (10 mM sodium
556 phosphate, 500 mM NaCl and 5 mM imidazole, pH 7.4). The pellet suspension was then
557 sonicated and spun down. Soluble proteins were purified using HisTrap^{TM} Excel (GE
558 Healthcare, Poland) column in buffer A with a linear gradient of 0-100% of 1 M imidazole in
559 buffer A in 20 column volumes. Fractions containing protein of interest were pooled together
560 and the buffer was exchanged to 50 mM Tris pH 7.5. Lastly, the protein of interest was purified
561 by ion-exchange chromatography using MonoQ 4.6/100 PE column (GE Healthcare, Poland)
562 with a linear gradient of 0-100% 50 mM Tris pH 7.5, 1M NaCl in 15 column volumes.
563
564 **Expression and purification of the HCoV-HKU1 Spike protein**
565 293T cells were seeded on 60 cm^2 dishes, cultured for 24 h at 37°C with 5% CO_2 and
566 transfected with 25 μg of pSecTag2-HKU-S plasmid per dish using polyethyleneimine (Sigma
567 Aldrich, Poland). Cells were further cultured for 72 h at 37°C with 5% CO_2 and collected for
568 HKU1-S purification. Cell pellets were lysed in RIPA buffer (50 mM Tris, 150 mM NaCl,
569 1% Nonidet P-40, 0.5% sodium deoxycholate, 0.1% SDS, pH 7.5) in the presence of Viscolase
570 (1250 U/ml; A&A Biotechnology, Poland), clarified by centrifugation, and filtered (0.45 μm
571 syringe PES filter). Supernatant containing 6 × His tagged S protein was mixed in 1:2 ratio with
572 binding buffer (20 mM NaH_2PO_4, 500 mM NaCl, 20 mM imidazole, pH = 7.4) and purified
573 using a fast performance liquid chromatography system (FPLC; AKTA, GE Healthcare,
574 Poland) with a Ni^{2+} HiTrap IMAC (2 × 1 ml) column (GE Healthcare, Poland) preequilibrated
575 with the binding buffer. The 6 × His tagged S protein was eluted with elution buffer (20 mM
576 NaH_2PO_4, 500 mM NaCl, 500 mM imidazole, pH = 6.9). The control sample from mock-
577 transfected cells was prepared in the same manner. Fractions containing 6 × His tagged
578 S protein or the respective fractions from control purification were pooled and dialyzed against
579 phosphate-buffered saline (PBS) with 5% glycerol.

580

581 **CleavEx screening assay and HKU1-S cleavage**

582 A total of 15 ng of each CleavEx protein was incubated with 50, 250 and 500 nM
583 KLK13, respectively in 50 mM Tris pH 7.5. For the full-length Spike protein, fractions
584 containing purified HKU1-S or mock samples were incubated with 0.5, 1.0 or 5.0 μM KLK13,
585 respectively in 50 mM Tris pH 7.5. Samples were incubated at 37°C for 3 hours and
586 immediately halted with the addition of 50 mM DTT-supplemented SDS sample buffer (1:1),
587 boiled for 5 min, cooled on ice, and separated on 10% polyacrylamide gels alongside dual-color
588 Page Ruler Prestained Protein size markers (Thermo Fisher Scientific, Poland). The separated
589 proteins were then transferred onto a Westran S PVDF membrane (GE Healthcare, Poland) by
590 wet blotting (Bio-Rad, Poland) for 1 h, 100 Volts in transfer buffer: 25 mM Tris, 192 mM
591 glycine, 20% methanol at 4°C. The membranes were then blocked by overnight incubation (at
592 4°C) in TBS-Tween (0.1%) buffer supplemented with 5% skimmed milk (BioShop, Canada).
593 A horseradish peroxidase-labeled anti-His tag antibody (1:25000 dilution; Sigma-Aldrich,
594 Poland) diluted in 5% skimmed milk / TBS-Tween (0.1%) was used to detect the His-tagged
595 HmuY proteins. The signal was developed using the Pierce ECL Western blotting substrate
596 (Thermo Scientific, Poland) and visualized using the ChemiDoc Imaging System (Bio-Rad,
597 Poland).

598

599 **Identification of the cleavage site**

600 A total of 10 μg S1/S2 CleavEx protein was incubated with 500 nM of KLK13 at 37°C
601 for 5 h. Next, the reaction was stopped by the addition of 50 mM DTT-supplemented SDS
602 sample buffer (1:1) and samples were immediately boiled for 5 min. The samples were then
603 separated on 10% polyacrylamide gel alongside the dual-color Page Ruler Prestained Protein
604 size markers (Thermo Fisher Scientific, Poland) in the Tris-Tricine SDS-PAGE system. The

605 separated proteins were then electrotransferred onto a Western S PVDF membrane (GE
606 Healthcare, Poland) using the Trans-Blot SD Semi-Dry Transfer Cell (Bio-Rad, Poland). The
607 transfer was performed for 30 min at 15 V in transfer buffer (10 mM N-cyclohexyl-3-
608 aminopropanesulfonic acid , 10% methanol, pH 11). Following the transfer, the membrane was
609 stained with 0.025% (w/v) Coomassie Brilliant Blue R-250 (BioShop, Poland) and the bands
610 of interest were sequenced *via* Edman degradation using a PPSQ-31A automatic protein
611 sequencer (Shimadzu, Japan).
612

TABLES

Table 1. KLKs inhibitors used in the study (*61*).

Protein	Inhibitor sequences
KLK7	Biotin-KTLF-CMK / Biotin-PEG-KTLF-CMK
KLK8	Biotin-TNKR-CMK / Biotin-PEG-TNKR-CMK
KLK13	Biotin-VRFR-CMK / Biotin-PEG-VRFR-CMK

Table 2. Primers used for generation of plasmid constructs.

Target/vector	Primer	Primer sequence (5'− 3')
KLK13/ pWPI	Sense	AGTCGTTTAAACGCCACCATGTGGCCCCTGGCCCTAGTGATCGCC
	Antisense	GATCGTTTAAACTTATTGTGGGCCCTTCAACCATTTTTG
TMPRSS2/ pWPI	Sense	AGTCGTTTAAACGCCACCATGGCTTTGAACTCAGGGTCACCA
	Antisense	GATCGTTTAAACTTAGCCGTCTGCCCTCATTTGTCGATAAATC
shRNA1 for KLK13/ pLKO.1-TRC	Sense	CCGGAACAGAACACTGTATGGCATCCTCGAGGATGCCATACAGTGTTCTGTTTTTTTG
	Antisense	AATTCAAAAAAACAGAACACTGTATGGCATCCTCGAGGATGCCATACAGTGTTCTGTT
shRNA2 for KLK13/ pLKO.1-TRC	Sense	CCGGAACTCTACAATGTGCCAACATCTCGAGATGTTGGCACATTGTAGAGTTTTTTTG
	Antisense	AATTCAAAAAAACTCTACAATGTGCCAACATCTCGAGATGTTGGCACATTGTAGAGTT
shRNA3 for KLK13/ pLKO.1-TRC	Sense	CCGGAACATGTTGTGTGCCGGCACACTCGAGTGTGCCGGCACACAACATGTTTTTTTG
	Antisense	AATTCAAAAAAACATGTTGTGTGCCGGCACACTCGAGTGTGCCGGCACACAACATGT
KLK13/ pLEXSY	Sense 1	GACGACGACAAGCTTGGTGACGTTGCCAATGCTGTG
	Sense 2	CCATCATCACCACGACGACGACGACAAGCTTGGTGACGTTG
	Sense 3	ATATCTAGACATCACCATCATCACCACGACGACGAC
	Antisense	ATAGCGGCCGCTTATTGTGGGCCCTTCAACCAT
HKU1-S/ pSecTag2	Sense	AGCTGGCCCAGCCGGCCCTGCTGATCATCTTCATCCTG
	Antisense	AGCTGCGGCCGCAGCGTAATCTGGAACATCGTATGGGTAGCTGTAGCCCTGGCGGACCC

618 **Table 3. Primers used for PCR of each KLK gene.**

Target	Primer	Primer sequence (5'− 3')
KLK1	Sense	CTCCTGGAGAACCACACCCGCC
	Antisense	GCGACAGAAGGCTTATTGGGGG
KLK2	Sense	GGCAGGTGGCTGTGTACAGTC
	Antisense	CAACATGAACTCTGTCACCTTCTC
KLK3	Sense	CGATATGAGCCTCCTGAAGAATC
	Antisense	TACCTTGAAGCACACCATTACA
KLK4	Sense	GCGGCACTGGTCATGGAAAACG
	Antisense	AACATGCTGGGGTGGTACAGCGG
KLK5	Sense	GTCACCAGTTTATGAATCTGGGC
	Antisense	GGCGCAGAACATGGTGTCATC
KLK6	Sense	GAAGCTGATGGTGGTGCTGAGTCTG
	Antisense	GTCAGGGAAATCACCATCTGCTGTC
KLK7	Sense	CCGCCCACTGCAAGATGAATGAG
	Antisense	AGCGCACAGCATGGAATTTTCC
KLK8	Sense	GCCTTGTTCCAGGGCCAGC
	Antisense	GCATCCTCACACTTCTTCTGGG
KLK9	Sense	TCTTCCCCCACCCTGGCTTCAAC
	Antisense	CGGGGTCTGGAGCAGGGCTCAG
KLK10	Sense	GGAAACAAGCCACTGTGGGC
	Antisense	GAGGATGCCTTGGAGGGTCTC
KLK11	Sense	CTCTGGCAACAGGGCTTGTAGGG
	Antisense	GCATCGCAAGGTGTGAGGCAGG
KLK12	Sense	TTGACCACAGGTGGGTCCTCA
	Antisense	GTGTAGACTCCAGGGATGCCA
KLK13	Sense	GGAGAAGCCCCACCCACCTG
	Antisense	CACGGATCCACAGGACGTATCTTG
KLK14	Sense	CACTGCGGCCGCCCGATC
	Antisense	GGCAGGGCGCAGCGCTCC
KLK15	Sense	CTACGGACCACGTCTCGGGTC
	Antisense	GACACCAGGCTTGGTGGTGTTG
β-actin	Sense	CCACACTGTGCCCATCTACG
	Antisense	AGGATCTTCATGAGGTAGTCAGTCAG

619 Primers for KLKs: 1, 2, 4-15 were acquired from (*99*). Primers for KLK3 were developed and
620 optimized in our laboratory.

621 **Table 4. Primers used in the CleavEx design.**

Target	Primer	Primer sequence (5'− 3')
proKLK13	Antisense	ATATGCGGCCGCTTATTTAACGGGGTATGTATAAGCGA
	Sense 1	TGCTGAACACCAACGACGAGCCGAACCAACCCT
	Sense 2	AAGCAGCAAAGTGCTGAACACCAACGACGAGCC
	Sense 3	ATATGTCGACCAGGAAAGCAGCAAAGTGCTGAACACCAAC
HKU1-S (S1/S2)	Antisense	GTCGACCTGCAGGCTCGC
	Sense	CGTAAACGTCGTTCTATCTCTGCGGACGAGCCGAACCAACCC
HKU1-S (S2/S2')	Antisense	GTCGACCTGCAGGCTCGC
	Sense	TCTTCTTCTCGTTCTTTTTTTGAAGACGAGCCGAACCAACCC

622

ACKNOWLEDGEMENTS

This work was supported by grants from the National Science Center UMO-2013/08/W/NZ1/00696 (J.P.), UMO-2016/22/E/NZ5/00332 (T.K.), UMO-2013/08/S/NZ6/00730 (A.N.), UMO-2012/07/E/NZ6/01712 and UMO-2017/27/B/NZ6/02488 (K.P.). Faculty of Biochemistry, Biophysics and Biotechnology of the Jagiellonian University is a partner of the Leading National Research Center supported by the Ministry of Science and Higher Education of the Republic of Poland. The authors are grateful to Xingchuan Huang for providing pCAGGS/HKU1-S plasmid, Ambra Saraccino for providing pWPI vector, Laura Sasiadek for providing KLK primers used in the study and Grzegorz Dubin for providing reference samples. The funders had no role in study design, data collection, and analysis, decision to publish, or preparation of the manuscript.

AUTHOR CONTRIBUTIONS STATEMENT

A.M., K.F., E.B., M.K, A.N. and P.M conducted the experiments. A.L., T.K., M.O., M.U. and J.P. provided materials and methods for the study. A.M. and K.P. designed the study and experiments, analyzed the data, and wrote the manuscript. K.P. and T.K. supervised the study. All authors reviewed the manuscript and approved the submitted version. All authors agreed to be personally accountable for their contributions and to ensure that questions related to the accuracy or integrity of any part of the work are appropriately investigated, resolved, and the resolution documented in the literature.

ADDITIONAL INFORMATION

Competing interests

The authors declare no competing financial interests.

REFERENCES

1. B. N. Fields, D. M. Knipe, P. M. Howley, *Fields virology*. (Wolters Kluwer Health/Lippincott Williams & Wilkins, Philadelphia, ed. 6th ed, 2013).
2. J. S. Peiris, K. Y. Yuen, A. D. Osterhaus, K. Stöhr, The severe acute respiratory syndrome. *N Engl J Med* **349**, 2431-2441 (2003); published online EpubDec (10.1056/NEJMra032498).
3. R. J. de Groot, S. C. Baker, R. S. Baric, C. S. Brown, C. Drosten, L. Enjuanes, R. A. Fouchier, M. Galiano, A. E. Gorbalenya, Z. A. Memish, S. Perlman, L. L. Poon, E. J. Snijder, G. M. Stephens, P. C. Woo, A. M. Zaki, M. Zambon, J. Ziebuhr, Middle East respiratory syndrome coronavirus (MERS-CoV): announcement of the Coronavirus Study Group. *J Virol* **87**, 7790-7792 (2013); published online EpubJul (10.1128/JVI.01244-13).
4. A. M. Zaki, S. van Boheemen, T. M. Bestebroer, A. D. Osterhaus, R. A. Fouchier, Isolation of a novel coronavirus from a man with pneumonia in Saudi Arabia. *N Engl J Med* **367**, 1814-1820 (2012); published online EpubNov 8 (10.1056/NEJMoa1211721).
5. L. van der Hoek, K. Pyrc, M. F. Jebbink, W. Vermeulen-Oost, R. J. Berkhout, K. C. Wolthers, P. M. Wertheim-van Dillen, J. Kaandorp, J. Spaargaren, B. Berkhout, Identification of a new human coronavirus. *Nat Med* **10**, 368-373 (2004); published online EpubApr (10.1038/nm1024).
6. L. van der Hoek, K. Sure, G. Ihorst, A. Stang, K. Pyrc, M. F. Jebbink, G. Petersen, J. Forster, B. Berkhout, K. Uberla, Croup is associated with the novel coronavirus NL63. *PLoS Med* **2**, e240 (2005); published online EpubAug (10.1371/journal.pmed.0020240).
7. C. L. Yeager, R. A. Ashmun, R. K. Williams, C. B. Cardellichio, L. H. Shapiro, A. T. Look, K. V. Holmes, Human aminopeptidase N is a receptor for human coronavirus 229E. *Nature* **357**, 420-422 (1992); published online EpubJun (10.1038/357420a0).
8. R. Dijkman, M. F. Jebbink, M. Deijs, A. Milewska, K. Pyrc, E. Buelow, A. van der Bijl, L. van der Hoek, Replication-dependent downregulation of cellular angiotensin-converting enzyme 2 protein expression by human coronavirus NL63. *J Gen Virol* **93**, 1924-1929 (2012); published online EpubSep (10.1099/vir.0.043919-0).
9. H. Hofmann, K. Pyrc, L. van der Hoek, M. Geier, B. Berkhout, S. Pöhlmann, Human coronavirus NL63 employs the severe acute respiratory syndrome coronavirus receptor for cellular entry. *Proc Natl Acad Sci U S A* **102**, 7988-7993 (2005); published online EpubMay (10.1073/pnas.0409465102).
10. S. Pöhlmann, T. Gramberg, A. Wegele, K. Pyrc, L. van der Hoek, B. Berkhout, H. Hofmann, Interaction between the spike protein of human coronavirus NL63 and its cellular receptor ACE2. *Adv Exp Med Biol* **581**, 281-284 (2006)10.1007/978-0-387-33012-9_47).
11. H. Hofmann, A. Marzi, T. Gramberg, M. Geier, K. Pyrc, L. van der Hoek, B. Berkhout, S. Pohlmann, Attachment factor and receptor engagement of SARS coronavirus and human coronavirus NL63. *Advances in experimental medicine and biology* **581**, 219-227 (2006)10.1007/978-0-387-33012-9_37).
12. A. Naskalska, A. Dabrowska, P. Nowak, A. Szczepanski, K. Jasik, A. Milewska, M. Ochman, S. Zeglen, Z. Rajfur, K. Pyrc, Novel coronavirus-like particles targeting cells lining the respiratory tract. *PLoS One* **13**, e0203489 (2018)10.1371/journal.pone.0203489).
13. A. Naskalska, A. Dabrowska, A. Szczepanski, A. Milewska, K. P. Jasik, K. Pyrc, Membrane protein of HCoV-NL63 is responsible for interaction with the adhesion receptor. *J Virol*, (2019); published online EpubJul 17 (10.1128/JVI.00355-19).
14. A. Milewska, M. Zarebski, P. Nowak, K. Stozek, J. Potempa, K. Pyrc, Human coronavirus NL63 utilizes heparan sulfate proteoglycans for attachment to target cells. *J Virol* **88**, 13221-13230 (2014); published online EpubNov (10.1128/JVI.02078-14).
15. W. Li, M. J. Moore, N. Vasilieva, J. Sui, S. K. Wong, M. A. Berne, M. Somasundaran, J. L. Sullivan, K. Luzuriaga, T. C. Greenough, H. Choe, M. Farzan, Angiotensin-converting enzyme 2 is a functional receptor for the SARS coronavirus. *Nature* **426**, 450-454 (2003); published online EpubNov (10.1038/nature02145).

16. V. S. Raj, H. Mou, S. L. Smits, D. H. Dekkers, M. A. Müller, R. Dijkman, D. Muth, J. A. Demmers, A. Zaki, R. A. Fouchier, V. Thiel, C. Drosten, P. J. Rottier, A. D. Osterhaus, B. J. Bosch, B. L. Haagmans, Dipeptidyl peptidase 4 is a functional receptor for the emerging human coronavirus-EMC. *Nature* **495**, 251-254 (2013); published online EpubMar (10.1038/nature12005).
17. R. Vlasak, W. Luytjes, W. Spaan, P. Palese, Human and bovine coronaviruses recognize sialic acid-containing receptors similar to those of influenza C viruses. *Proc Natl Acad Sci U S A* **85**, 4526-4529 (1988); published online EpubJun (
18. A. Szczepanski, K. Owczarek, M. Bzowska, K. Gula, I. Drebot, M. Ochman, B. Maksym, Z. Rajfur, J. A. Mitchell, K. Pyrc, Canine Respiratory Coronavirus, Bovine Coronavirus, and Human Coronavirus OC43: Receptors and Attachment Factors. *Viruses* **11**, (2019); published online EpubApr (10.3390/v11040328).
19. P. C. Woo, S. K. Lau, C. M. Chu, K. H. Chan, H. W. Tsoi, Y. Huang, B. H. Wong, R. W. Poon, J. J. Cai, W. K. Luk, L. L. Poon, S. S. Wong, Y. Guan, J. S. Peiris, K. Y. Yuen, Characterization and complete genome sequence of a novel coronavirus, coronavirus HKU1, from patients with pneumonia. *J Virol* **79**, 884-895 (2005); published online EpubJan (10.1128/JVI.79.2.884-895.2005).
20. S. R. Dominguez, C. C. Robinson, K. V. Holmes, Detection of four human coronaviruses in respiratory infections in children: a one-year study in Colorado. *J Med Virol* **81**, 1597-1604 (2009); published online EpubSep (10.1002/jmv.21541).
21. W. Zhou, W. Wang, H. Wang, R. Lu, W. Tan, First infection by all four non-severe acute respiratory syndrome human coronaviruses takes place during childhood. *BMC Infect Dis* **13**, 433 (2013); published online EpubSep (10.1186/1471-2334-13-433).
22. R. Dijkman, M. F. Jebbink, S. M. Koekkoek, M. Deijs, H. R. Jónsdóttir, R. Molenkamp, M. Ieven, H. Goossens, V. Thiel, L. van der Hoek, Isolation and characterization of current human coronavirus strains in primary human epithelial cell cultures reveal differences in target cell tropism. *J Virol* **87**, 6081-6090 (2013); published online EpubJun (10.1128/JVI.03368-12).
23. S. R. Dominguez, S. Shrivastava, A. Berglund, Z. Qian, L. G. Góes, R. A. Halpin, N. Fedorova, A. Ransier, P. A. Weston, E. L. Durigon, J. A. Jerez, C. C. Robinson, C. D. Town, K. V. Holmes, Isolation, propagation, genome analysis and epidemiology of HKU1 betacoronaviruses. *J Gen Virol* **95**, 836-848 (2014); published online EpubApr (10.1099/vir.0.059832-0).
24. S. R. Dominguez, E. A. Travanty, Z. Qian, R. J. Mason, Human coronavirus HKU1 infection of primary human type II alveolar epithelial cells: cytopathic effects and innate immune response. *PLoS One* **8**, e70129 (2013)10.1371/journal.pone.0070129).
25. K. Pyrc, A. C. Sims, R. Dijkman, M. Jebbink, C. Long, D. Deming, E. Donaldson, A. Vabret, R. Baric, L. van der Hoek, R. Pickles, Culturing the unculturable: human coronavirus HKU1 infects, replicates, and produces progeny virions in human ciliated airway epithelial cell cultures. *J Virol* **84**, 11255-11263 (2010); published online EpubNov (10.1128/JVI.00947-10).
26. X. Huang, W. Dong, A. Milewska, A. Golda, Y. Qi, Q. K. Zhu, W. A. Marasco, R. S. Baric, A. C. Sims, K. Pyrc, W. Li, J. Sui, Human Coronavirus HKU1 Spike Protein Uses O-Acetylated Sialic Acid as an Attachment Receptor Determinant and Employs Hemagglutinin-Esterase Protein as a Receptor-Destroying Enzyme. *J Virol* **89**, 7202-7213 (2015); published online EpubJul (10.1128/JVI.00854-15).
27. M. J. Bakkers, Y. Lang, L. J. Feitsma, R. J. Hulswit, S. A. de Poot, A. L. van Vliet, I. Margine, J. D. de Groot-Mijnes, F. J. van Kuppeveld, M. A. Langereis, E. G. Huizinga, R. J. de Groot, Betacoronavirus Adaptation to Humans Involved Progressive Loss of Hemagglutinin-Esterase Lectin Activity. *Cell Host Microbe* **21**, 356-366 (2017); published online EpubMar 8 (10.1016/j.chom.2017.02.008).
28. R. J. G. Hulswit, Y. Lang, M. J. G. Bakkers, W. Li, Z. Li, A. Schouten, B. Ophorst, F. J. M. van Kuppeveld, G. J. Boons, B. J. Bosch, E. G. Huizinga, R. J. de Groot, Human coronaviruses OC43 and HKU1 bind to 9-. *Proc Natl Acad Sci U S A* **116**, 2681-2690 (2019); published online EpubFeb (10.1073/pnas.1809667116).

29. T. M. Gallagher, C. Escarmis, M. J. Buchmeier, Alteration of the pH dependence of coronavirus-induced cell fusion: effect of mutations in the spike glycoprotein. *J Virol* **65**, 1916-1928 (1991); published online EpubApr (
30. R. Nomura, A. Kiyota, E. Suzaki, K. Kataoka, Y. Ohe, K. Miyamoto, T. Senda, T. Fujimoto, Human coronavirus 229E binds to CD13 in rafts and enters the cell through caveolae. *J Virol* **78**, 8701-8708 (2004); published online EpubAug (10.1128/JVI.78.16.8701-8708.2004).
31. Y. Inoue, N. Tanaka, Y. Tanaka, S. Inoue, K. Morita, M. Zhuang, T. Hattori, K. Sugamura, Clathrin-dependent entry of severe acute respiratory syndrome coronavirus into target cells expressing ACE2 with the cytoplasmic tail deleted. *J Virol* **81**, 8722-8729 (2007); published online EpubAug (10.1128/JVI.00253-07).
32. E. Van Hamme, H. L. Dewerchin, E. Cornelissen, B. Verhasselt, H. J. Nauwynck, Clathrin- and caveolae-independent entry of feline infectious peritonitis virus in monocytes depends on dynamin. *J Gen Virol* **89**, 2147-2156 (2008); published online EpubSep (10.1099/vir.0.2008/001602-0).
33. H. Wang, P. Yang, K. Liu, F. Guo, Y. Zhang, G. Zhang, C. Jiang, SARS coronavirus entry into host cells through a novel clathrin- and caveolae-independent endocytic pathway. *Cell Res* **18**, 290-301 (2008); published online EpubFeb (10.1038/cr.2008.15).
34. A. Milewska, P. Nowak, K. Owczarek, A. Szczepanski, M. Zarebski, A. Hoang, K. Berniak, J. Wojarski, S. Zeglen, Z. Baster, Z. Rajfur, K. Pyrc, Entry of Human Coronavirus NL63 into the Cell. *J Virol* **92**, (2018); published online EpubFeb (10.1128/JVI.01933-17).
35. K. Owczarek, A. Szczepanski, A. Milewska, Z. Baster, Z. Rajfur, M. Sarna, K. Pyrc, Early events during human coronavirus OC43 entry to the cell. *Sci Rep* **8**, 7124 (2018); published online EpubMay 8 (10.1038/s41598-018-25640-0).
36. J. E. Park, D. J. Cruz, H. J. Shin, Receptor-bound porcine epidemic diarrhea virus spike protein cleaved by trypsin induces membrane fusion. *Arch Virol* **156**, 1749-1756 (2011); published online EpubOct (10.1007/s00705-011-1044-6).
37. C. A. de Haan, B. J. Haijema, P. Schellen, P. Wichgers Schreur, E. te Lintelo, H. Vennema, P. J. Rottier, Cleavage of group 1 coronavirus spike proteins: how furin cleavage is traded off against heparan sulfate binding upon cell culture adaptation. *J Virol* **82**, 6078-6083 (2008); published online EpubJun (10.1128/JVI.00074-08).
38. R. N. Kirchdoerfer, C. A. Cottrell, N. Wang, J. Pallesen, H. M. Yassine, H. L. Turner, K. S. Corbett, B. S. Graham, J. S. McLellan, A. B. Ward, Pre-fusion structure of a human coronavirus spike protein. *Nature* **531**, 118-121 (2016); published online EpubMar (10.1038/nature17200).
39. C. A. de Haan, K. Stadler, G. J. Godeke, B. J. Bosch, P. J. Rottier, Cleavage inhibition of the murine coronavirus spike protein by a furin-like enzyme affects cell-cell but not virus-cell fusion. *J Virol* **78**, 6048-6054 (2004); published online EpubJun (10.1128/JVI.78.11.6048-6054.2004).
40. J. K. Millet, G. R. Whittaker, Host cell entry of Middle East respiratory syndrome coronavirus after two-step, furin-mediated activation of the spike protein. *Proc Natl Acad Sci U S A* **111**, 15214-15219 (2014); published online EpubOct (10.1073/pnas.1407087111).
41. Y. Yamada, D. X. Liu, Proteolytic activation of the spike protein at a novel RRRR/S motif is implicated in furin-dependent entry, syncytium formation, and infectivity of coronavirus infectious bronchitis virus in cultured cells. *J Virol* **83**, 8744-8758 (2009); published online EpubSep (10.1128/JVI.00613-09).
42. Y. W. Kam, Y. Okumura, H. Kido, L. F. Ng, R. Bruzzone, R. Altmeyer, Cleavage of the SARS coronavirus spike glycoprotein by airway proteases enhances virus entry into human bronchial epithelial cells in vitro. *PLoS One* **4**, e7870 (2009); published online EpubNov (10.1371/journal.pone.0007870).
43. M. Kawase, K. Shirato, S. Matsuyama, F. Taguchi, Protease-mediated entry via the endosome of human coronavirus 229E. *J Virol* **83**, 712-721 (2009); published online EpubJan (10.1128/JVI.01933-08).

44. Z. Qiu, S. T. Hingley, G. Simmons, C. Yu, J. Das Sarma, P. Bates, S. R. Weiss, Endosomal proteolysis by cathepsins is necessary for murine coronavirus mouse hepatitis virus type 2 spike-mediated entry. *J Virol* **80**, 5768-5776 (2006); published online EpubJun (10.1128/JVI.00442-06).
45. K. Shirato, M. Kawase, S. Matsuyama, Middle East respiratory syndrome coronavirus infection mediated by the transmembrane serine protease TMPRSS2. *J Virol* **87**, 12552-12561 (2013); published online EpubDec (10.1128/JVI.01890-13).
46. G. Simmons, D. N. Gosalia, A. J. Rennekamp, J. D. Reeves, S. L. Diamond, P. Bates, Inhibitors of cathepsin L prevent severe acute respiratory syndrome coronavirus entry. *Proc Natl Acad Sci U S A* **102**, 11876-11881 (2005); published online EpubAug (10.1073/pnas.0505577102).
47. S. Bertram, R. Dijkman, M. Habjan, A. Heurich, S. Gierer, I. Glowacka, K. Welsch, M. Winkler, H. Schneider, H. Hofmann-Winkler, V. Thiel, S. Pohlmann, TMPRSS2 activates the human coronavirus 229E for cathepsin-independent host cell entry and is expressed in viral target cells in the respiratory epithelium. *J Virol* **87**, 6150-6160 (2013); published online EpubJun (10.1128/JVI.03372-12).
48. S. Gierer, S. Bertram, F. Kaup, F. Wrensch, A. Heurich, A. Kramer-Kuhl, K. Welsch, M. Winkler, B. Meyer, C. Drosten, U. Dittmer, T. von Hahn, G. Simmons, H. Hofmann, S. Pohlmann, The spike protein of the emerging betacoronavirus EMC uses a novel coronavirus receptor for entry, can be activated by TMPRSS2, and is targeted by neutralizing antibodies. *J Virol* **87**, 5502-5511 (2013); published online EpubMay (10.1128/JVI.00128-13).
49. I. Glowacka, S. Bertram, M. A. Muller, P. Allen, E. Soilleux, S. Pfefferle, I. Steffen, T. S. Tsegaye, Y. He, K. Gnirss, D. Niemeyer, H. Schneider, C. Drosten, S. Pohlmann, Evidence that TMPRSS2 activates the severe acute respiratory syndrome coronavirus spike protein for membrane fusion and reduces viral control by the humoral immune response. *J Virol* **85**, 4122-4134 (2011); published online EpubMay (10.1128/JVI.02232-10).
50. K. Shirato, S. Matsuyama, M. Ujike, F. Taguchi, Role of proteases in the release of porcine epidemic diarrhea virus from infected cells. *J Virol* **85**, 7872-7880 (2011); published online EpubAug (10.1128/JVI.00464-11).
51. K. Shirato, M. Kawase, S. Matsuyama, Wild-type human coronaviruses prefer cell-surface TMPRSS2 to endosomal cathepsins for cell entry. *Virology* **517**, 9-15 (2018); published online Epub04 (10.1016/j.virol.2017.11.012).
52. T. J. Harvey, J. D. Hooper, S. A. Myers, S. A. Stephenson, L. K. Ashworth, J. A. Clements, Tissue-specific expression patterns and fine mapping of the human kallikrein (KLK) locus on proximal 19q13.4. *J Biol Chem* **275**, 37397-37406 (2000); published online EpubDec (10.1074/jbc.M004525200).
53. J. L. Shaw, E. P. Diamandis, Distribution of 15 human kallikreins in tissues and biological fluids. *Clin Chem* **53**, 1423-1432 (2007); published online EpubAug (10.1373/clinchem.2007.088104).
54. N. Emami, E. P. Diamandis, New insights into the functional mechanisms and clinical applications of the kallikrein-related peptidase family. *Mol Oncol* **1**, 269-287 (2007); published online EpubDec (10.1016/j.molonc.2007.09.003).
55. J. Clements, J. Hooper, Y. Dong, T. Harvey, The expanded human kallikrein (KLK) gene family: genomic organisation, tissue-specific expression and potential functions. *Biol Chem* **382**, 5-14 (2001); published online EpubJan (10.1515/BC.2001.002).
56. M. Kalinska, U. Meyer-Hoffert, T. Kantyka, J. Potempa, Kallikreins - The melting pot of activity and function. *Biochimie* **122**, 270-282 (2016); published online EpubMar (10.1016/j.biochi.2015.09.023).
57. N. Memari, L. Grass, T. Nakamura, I. Karakucuk, E. P. Diamandis, Human tissue kallikrein 9: production of recombinant proteins and specific antibodies. *Biol Chem* **387**, 733-740 (2006); published online EpubJun (10.1515/BC.2006.092).

58. N. Memari, W. Jiang, E. P. Diamandis, L. Y. Luo, Enzymatic properties of human kallikrein-related peptidase 12 (KLK12). *Biol Chem* **388**, 427-435 (2007); published online EpubApr (10.1515/BC.2007.049).
59. M. R. Darling, L. Jackson-Boeters, T. D. Daley, E. P. Diamandis, Human kallikrein 13 expression in salivary gland tumors. *Int J Biol Markers* **21**, 106-110 (2006); published online Epub2006 Apr-Jun (
60. G. Sotiropoulou, G. Pampalakis, E. P. Diamandis, Functional roles of human kallikrein-related peptidases. *J Biol Chem* **284**, 32989-32994 (2009); published online EpubNov (10.1074/jbc.R109.027946).
61. N. Gruba, E. Bielecka, M. Wysocka, A. Wojtysiak, M. Brzezińska-Bodal, K. Sychowska, M. Kalińska, M. Magoch, A. Pęcak, K. Falkowski, M. Wiśniewska, L. Sąsiadek, K. Płaza, E. Kroll, A. Pejkovska, M. Rehders, K. Brix, G. Dubin, T. Kantyka, J. Potempa, A. Lesner, Development of Chemical Tools to Monitor Human Kallikrein 13 (KLK13) Activity. *Int J Mol Sci* **20**, (2019); published online EpubMar (10.3390/ijms20071557).
62. U. Meyer-Hoffert, Z. Wu, T. Kantyka, J. Fischer, T. Latendorf, B. Hansmann, J. Bartels, Y. He, R. Gläser, J. M. Schröder, Isolation of SPINK6 in human skin: selective inhibitor of kallikrein-related peptidases. *J Biol Chem* **285**, 32174-32181 (2010); published online EpubOct (10.1074/jbc.M109.091850).
63. T. Kantyka, J. Fischer, Z. Wu, W. Declercq, K. Reiss, J. M. Schröder, U. Meyer-Hoffert, Inhibition of kallikrein-related peptidases by the serine protease inhibitor of Kazal-type 6. *Peptides* **32**, 1187-1192 (2011); published online EpubJun (10.1016/j.peptides.2011.03.009).
64. C. Liu, Y. Ma, Y. Yang, Y. Zheng, J. Shang, Y. Zhou, S. Jiang, L. Du, J. Li, F. Li, Cell Entry of Porcine Epidemic Diarrhea Coronavirus Is Activated by Lysosomal Proteases. *J Biol Chem* **291**, 24779-24786 (2016); published online EpubNov 18 (10.1074/jbc.M116.740746).
65. X. Ou, H. Guan, B. Qin, Z. Mu, J. A. Wojdyla, M. Wang, S. R. Dominguez, Z. Qian, S. Cui, Crystal structure of the receptor binding domain of the spike glycoprotein of human betacoronavirus HKU1. *Nat Commun* **8**, 15216 (2017); published online EpubMay (10.1038/ncomms15216).
66. I. E. Ekholm, M. Brattsand, T. Egelrud, Stratum corneum tryptic enzyme in normal epidermis: a missing link in the desquamation process? *J Invest Dermatol* **114**, 56-63 (2000); published online EpubJan (10.1046/j.1523-1747.2000.00820.x).
67. A. Lundström, T. Egelrud, Stratum corneum chymotryptic enzyme: a proteinase which may be generally present in the stratum corneum and with a possible involvement in desquamation. *Acta Derm Venereol* **71**, 471-474 (1991).
68. J. D. Bartlett, Dental enamel development: proteinases and their enamel matrix substrates. *ISRN Dent* **2013**, 684607 (2013); published online EpubSep (10.1155/2013/684607).
69. A. Cho, N. Haruyama, B. Hall, M. J. Danton, L. Zhang, P. Arany, D. J. Mooney, Y. Harichane, M. Goldberg, C. W. Gibson, A. B. Kulkarni, TGF-ß regulates enamel mineralization and maturation through KLK4 expression. *PLoS One* **8**, e82267 (2013)10.1371/journal.pone.0082267).
70. P. S. Hart, T. C. Hart, M. D. Michalec, O. H. Ryu, D. Simmons, S. Hong, J. T. Wright, Mutation in kallikrein 4 causes autosomal recessive hypomaturation amelogenesis imperfecta. *J Med Genet* **41**, 545-549 (2004); published online EpubJul (
71. P. Papagerakis, G. Pannone, L. I. Zheng, M. Athanassiou-Papaefthymiou, Y. Yamakoshi, H. S. McGuff, O. Shkeir, K. Ghirtis, S. Papagerakis, Clinical significance of kallikrein-related peptidase-4 in oral cancer. *Anticancer Res* **35**, 1861-1866 (2015); published online EpubApr (
72. X. Charest-Morin, A. Raghavan, M. L. Charles, T. Kolodka, J. Bouthillier, M. Jean, M. S. Robbins, F. Marceau, Pharmacological effects of recombinant human tissue kallikrein on bradykinin B2 receptors. *Pharmacol Res Perspect* **3**, e00119 (2015); published online EpubMar (10.1002/prp2.119).
73. Y. Wang, W. Luo, G. Reiser, Trypsin and trypsin-like proteases in the brain: proteolysis and cellular functions. *Cell Mol Life Sci* **65**, 237-252 (2008); published online EpubJan (10.1007/s00018-007-7288-3).

74. K. Ogawa, T. Yamada, Y. Tsujioka, J. Taguchi, M. Takahashi, Y. Tsuboi, Y. Fujino, M. Nakajima, T. Yamamoto, H. Akatsu, S. Mitsui, N. Yamaguchi, Localization of a novel type trypsin-like serine protease, neurosin, in brain tissues of Alzheimer's disease and Parkinson's disease. *Psychiatry Clin Neurosci* **54**, 419-426 (2000); published online EpubAug (10.1046/j.1440-1819.2000.00731.x).
75. J. Lou, H. Si, Y. Chen, X. Sun, H. Zhang, A. Niu, C. Hu, Correlation between KLK6 expression and the clinicopathological features of glioma. *Contemp Oncol (Pozn)* **18**, 246-251 (2014)10.5114/wo.2014.44628).
76. C. Cerqueira, P. Samperio Ventayol, C. Vogeley, M. Schelhaas, Kallikrein-8 Proteolytically Processes Human Papillomaviruses in the Extracellular Space To Facilitate Entry into Host Cells. *J Virol* **89**, 7038-7052 (2015); published online EpubJul (10.1128/JVI.00234-15).
77. B. S. Hamilton, G. R. Whittaker, Cleavage activation of human-adapted influenza virus subtypes by kallikrein-related peptidases 5 and 12. *J Biol Chem* **288**, 17399-17407 (2013); published online EpubJun (10.1074/jbc.M112.440362).
78. M. Magnen, F. Gueugnon, A. Guillon, T. Baranek, V. C. Thibault, A. Petit-Courty, S. J. de Veer, J. Harris, A. A. Humbles, M. Si-Tahar, Y. Courty, Kallikrein-Related Peptidase 5 Contributes to H3N2 Influenza Virus Infection in Human Lungs. *J Virol* **91**, (2017); published online EpubAug (10.1128/JVI.00421-17).
79. J. Gibo, T. Ito, K. Kawabe, T. Hisano, M. Inoue, N. Fujimori, T. Oono, Y. Arita, H. Nawata, Camostat mesilate attenuates pancreatic fibrosis via inhibition of monocytes and pancreatic stellate cells activity. *Lab Invest* **85**, 75-89 (2005); published online EpubJan (10.1038/labinvest.3700203).
80. Y. Zhou, P. Vedantham, K. Lu, J. Agudelo, R. Carrion, J. W. Nunneley, D. Barnard, S. Pöhlmann, J. H. McKerrow, A. R. Renslo, G. Simmons, Protease inhibitors targeting coronavirus and filovirus entry. *Antiviral Res* **116**, 76-84 (2015); published online EpubApr (10.1016/j.antiviral.2015.01.011).
81. S. Matsuyama, K. Shirato, M. Kawase, Y. Terada, K. Kawachi, S. Fukushi, W. Kamitani, Middle East respiratory syndrome coronavirus spike protein is not activated directly by cellular furin during viral entry into target cells. *J Virol*, (2018); published online EpubJul (10.1128/JVI.00683-18).
82. L. R. de Souza, P. M Melo, T. Paschoalin, A. K. Carmona, M. Kondo, I. Y. Hirata, M. Blaber, I. Tersariol, J. Takatsuka, M. A. Juliano, L. Juliano, R. A. Gomes, L. Puzer, Human tissue kallikreins 3 and 5 can act as plasminogen activator releasing active plasmin. *Biochem Biophys Res Commun* **433**, 333-337 (2013); published online EpubApr (10.1016/j.bbrc.2013.03.001).
83. D. Andrade, D. M. Assis, J. A. Santos, F. M. Alves, I. Y. Hirata, M. S. Araujo, S. I. Blaber, M. Blaber, M. A. Juliano, L. Juliano, Substrate specificity of kallikrein-related peptidase 13 activated by salts or glycosaminoglycans and a search for natural substrate candidates. *Biochimie* **93**, 1701-1709 (2011); published online EpubOct (10.1016/j.biochi.2011.05.037).
84. M. G. Lawrence, J. Lai, J. A. Clements, Kallikreins on steroids: structure, function, and hormonal regulation of prostate-specific antigen and the extended kallikrein locus. *Endocr Rev* **31**, 407-446 (2010); published online EpubAug (10.1210/er.2009-0034).
85. A. Magklara, L. Grass, E. P. Diamandis, Differential steroid hormone regulation of human glandular kallikrein (hK2) and prostate-specific antigen (PSA) in breast cancer cell lines. *Breast Cancer Res Treat* **59**, 263-270 (2000); published online EpubFeb (
86. S. Morizane, K. Yamasaki, F. D. Kabigting, R. L. Gallo, Kallikrein expression and cathelicidin processing are independently controlled in keratinocytes by calcium, vitamin D(3), and retinoic acid. *J Invest Dermatol* **130**, 1297-1306 (2010); published online EpubMay (10.1038/jid.2009.435).
87. K. Oikonomopoulou, K. K. Hansen, M. Saifeddine, N. Vergnolle, I. Tea, M. Blaber, S. I. Blaber, I. Scarisbrick, E. P. Diamandis, M. D. Hollenberg, Kallikrein-mediated cell signalling: targeting

proteinase-activated receptors (PARs). *Biol Chem* **387**, 817-824 (2006); published online EpubJun (10.1515/BC.2006.104).

88. M. D. Hollenberg, K. Oikonomopoulou, K. K. Hansen, M. Saifeddine, R. Ramachandran, E. P. Diamandis, Kallikreins and proteinase-mediated signaling: proteinase-activated receptors (PARs) and the pathophysiology of inflammatory diseases and cancer. *Biol Chem* **389**, 643-651 (2008); published online EpubJun (10.1515/BC.2008.077).

89. K. Oikonomopoulou, K. K. Hansen, M. Saifeddine, I. Tea, M. Blaber, S. I. Blaber, I. Scarisbrick, P. Andrade-Gordon, G. S. Cottrell, N. W. Bunnett, E. P. Diamandis, M. D. Hollenberg, Proteinase-activated receptors, targets for kallikrein signaling. *J Biol Chem* **281**, 32095-32112 (2006); published online EpubOct (10.1074/jbc.M513138200).

90. A. Seliga, M. H. Lee, N. C. Fernandes, V. Zuluaga-Ramirez, M. Didukh, Y. Persidsky, R. Potula, S. Gallucci, U. Sriram, Kallikrein-Kinin System Suppresses Type I Interferon Responses: A Novel Pathway of Interferon Regulation. *Front Immunol* **9**, 156 (2018)10.3389/fimmu.2018.00156).

91. C. D. Petraki, P. A. Papanastasiou, V. N. Karavana, E. P. Diamandis, Cellular distribution of human tissue kallikreins: immunohistochemical localization. *Biol Chem* **387**, 653-663 (2006); published online EpubJun (10.1515/BC.2006.084).

92. T. Heald-Sargent, T. Gallagher, Ready, set, fuse! The coronavirus spike protein and acquisition of fusion competence. *Viruses* **4**, 557-580 (2012); published online Epub04 (10.3390/v4040557).

93. J. T. Earnest, M. P. Hantak, K. Li, P. B. McCray, S. Perlman, T. Gallagher, The tetraspanin CD9 facilitates MERS-coronavirus entry by scaffolding host cell receptors and proteases. *PLoS Pathog* **13**, e1006546 (2017); published online EpubJul (10.1371/journal.ppat.1006546).

94. J. Moffat, D. A. Grueneberg, X. Yang, S. Y. Kim, A. M. Kloepfer, G. Hinkle, B. Piqani, T. M. Eisenhaure, B. Luo, J. K. Grenier, A. E. Carpenter, S. Y. Foo, S. A. Stewart, B. R. Stockwell, N. Hacohen, W. C. Hahn, E. S. Lander, D. M. Sabatini, D. E. Root, A lentiviral RNAi library for human and mouse genes applied to an arrayed viral high-content screen. *Cell* **124**, 1283-1298 (2006); published online EpubMar (10.1016/j.cell.2006.01.040).

95. A. Horani, A. Nath, M. G. Wasserman, T. Huang, S. L. Brody, Rho-associated protein kinase inhibition enhances airway epithelial Basal-cell proliferation and lentivirus transduction. *Am J Respir Cell Mol Biol* **49**, 341-347 (2013); published online EpubSep (10.1165/rcmb.2013-0046TE).

96. A. Milewska, J. Ciejka, K. Kaminski, A. Karewicz, D. Bielska, S. Zeglen, W. Karolak, M. Nowakowska, J. Potempa, B. J. Bosch, K. Pyrc, K. Szczubialka, Novel polymeric inhibitors of HCoV-NL63. *Antiviral research* **97**, 112-121 (2013); published online EpubFeb (10.1016/j.antiviral.2012.11.006).

97. J. R. Kovalski, A. Bhaduri, A. M. Zehnder, P. H. Neela, Y. Che, G. G. Wozniak, P. A. Khavari, The Functional Proximal Proteome of Oncogenic Ras Includes mTORC2. *Mol Cell* **73**, 830-844.e812 (2019); published online Epub02 (10.1016/j.molcel.2018.12.001).

98. A. Milewska, K. Kaminski, J. Ciejka, K. Kosowicz, S. Zeglen, J. Wojarski, M. Nowakowska, K. Szczubiałka, K. Pyrc, HTCC: Broad Range Inhibitor of Coronavirus Entry. *PLoS One* **11**, e0156552 (2016)10.1371/journal.pone.0156552).

99. A. J. Lizama, Y. Andrade, P. Colivoro, J. Sarmiento, C. E. Matus, C. B. Gonzalez, K. D. Bhoola, P. Ehrenfeld, C. D. Figueroa, Expression and bioregulation of the kallikrein-related peptidases family in the human neutrophil. *Innate Immun* **21**, 575-586 (2015); published online EpubAug (10.1177/1753425914566083).

1003 **FIGURE TITLES AND LEGENDS**

1004 **FIGURE 1.**

1005

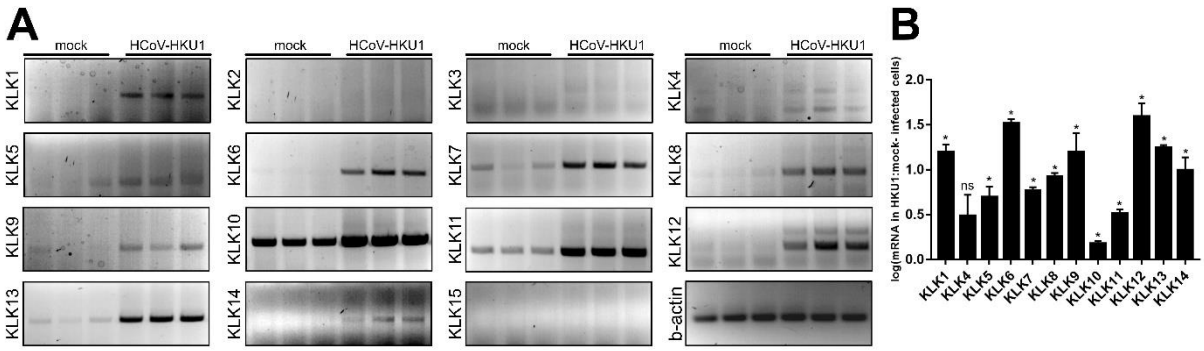

1006

1007 **Figure 1. Up-regulation of several KLKs after HCoV-HKU1 infection in HAE.**
1008 HAE cultures were infected with HCoV-HKU1 (10^6 RNA copies per ml) or mock for 2 h at
1009 32°C and cultured for 5 days. Cellular RNA was isolated, treated with DNase, reverse
1010 transcribed and each KLKs mRNA was amplified using specific primers. The analysis was
1011 performed two times using cells obtained from different donors, each time in triplicate. (**A**)
1012 Amplified PCR products were resolved and detected in 1.5% (w:v) agarose gel in 1 × TAE
1013 buffer. (**B**) The expression of each KLK comparing to β-actin control was assessed semi-
1014 quantitively by densitometry and is presented as a log change of signal specific for KLKs
1015 mRNA in HCoV-HKU1-infected cells, compared to the mock-infected cells. The experiment
1016 was performed three times using cells from different donors, each time with three biological
1017 replicates. For comparisons by Student's t-test, *Indicates $P < 0.05$; ns, not significant.

1018 **FIGURE 2.**

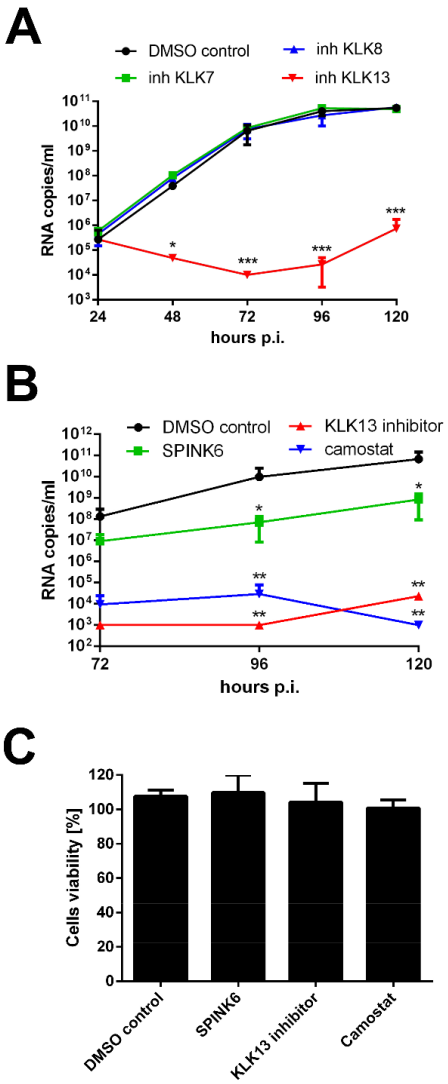

1019

1020 **Figure 2. HCoV-HKU1 infection is dependent on KLK13 activity.**

1021 HAE cultures were inoculated with HCoV-HKU1 (10^6 RNA copies per ml) for 2 h at 32°C in
1022 the presence of 10 µM KLKs inhibitors (**Table 1**) or DMSO (**A**); 10 µg/ml SPINK6, 10 µM
1023 KLK13 inhibitor, 100 µM camostat or DMSO (**B**). To analyze virus replication kinetics, each
1024 day post-infection, 100 µl of 1 × PBS with a given inhibitor was applied to the apical surface
1025 of HAE cultures and collected after 10 min incubation at 32°C. Replication of HCoV-HKU1
1026 was evaluated using an RT-qPCR and the data are presented as RNA copy number per ml. The
1027 assay was performed twice, each time in triplicate, and average values with standard errors are
1028 presented. Statistical significance was assessed with the Student's t-test, and the asterisks
1029 indicate: * $P < 0.05$, ** $P < 0.005$, *** $P < 0.0005$. (**C**) Cytotoxicity of inhibitors in HAE
1030 cultures. Cell viability was assessed with the XTT assay on mock-treated cells at 120 h post-
1031 infection. Data on the y-axis represent the percentage values obtained for the untreated
1032 reference samples. The assay was performed in triplicate and average values with standard
1033 errors are presented.

1034 **FIGURE 3.**

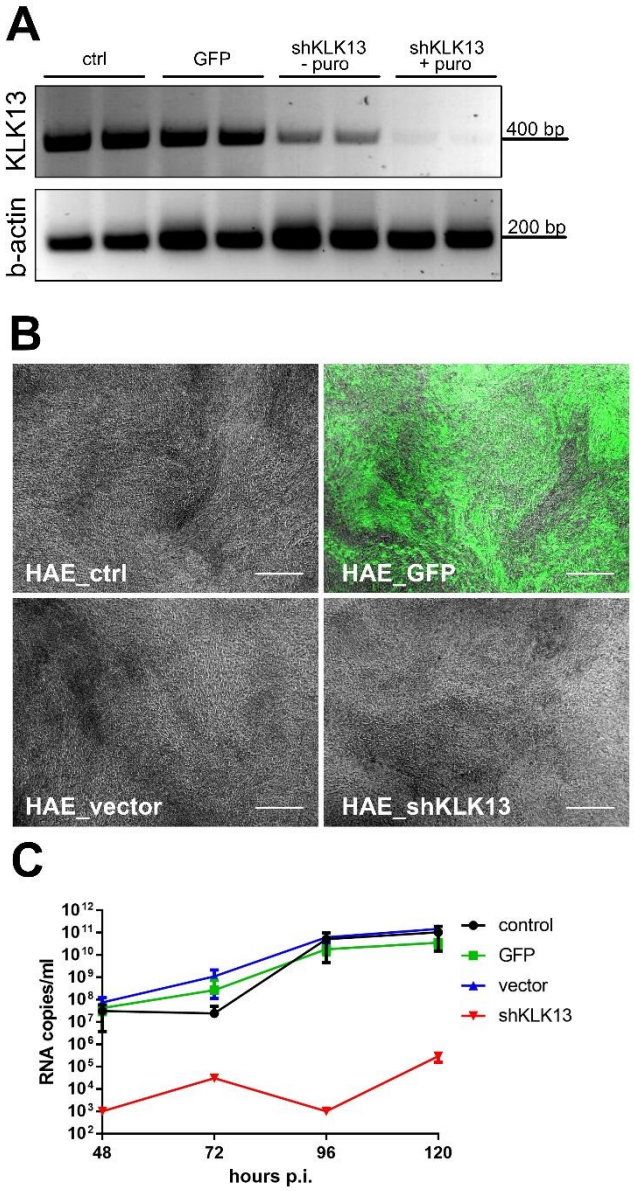

1035

1036 **Figure 3. HCoV-HKU1 does not replicate in HAE cells deficient in KLK13.**

1037 Primary human epithelial cells were transduced with lentiviral vectors harboring the GFP
1038 (HAE_GFP) protein, empty pLKO.1-TRC vector (HAE_vector) or shRNA for KLK13 mRNA
1039 (HAE_shKLK13). As a control, not transduced HAE cultures were used (HAE_ctrl). (**A**) The
1040 KLK13 mRNA was evaluated before (- puro) and after puromycin (+ puro) selection of
1041 positively transduced cells, β-actin was used as an internal control. (**B**) Microscopic
1042 examination of all HAE cultures after 4 weeks culture in ALI at 37°C. Scale bar = 200 μm. (**C**)
1043 All HAE cultures were inoculated with HCoV-HKU1 (10^6 RNA copies per ml) for 2 h at 32°C
1044 and cultured for 5 days. Each day post-infection, 100 μl of 1 × PBS was applied to the apical
1045 surface of HAE cultures and collected after 10 min incubation at 32°C. Replication of HCoV-
1046 HKU1 was evaluated using an RT-qPCR and the data are presented as RNA copy number per
1047 ml. The assay was performed twice, each time in triplicate, and average values with standard
1048 errors are presented.

1049 **FIGURE 4.**

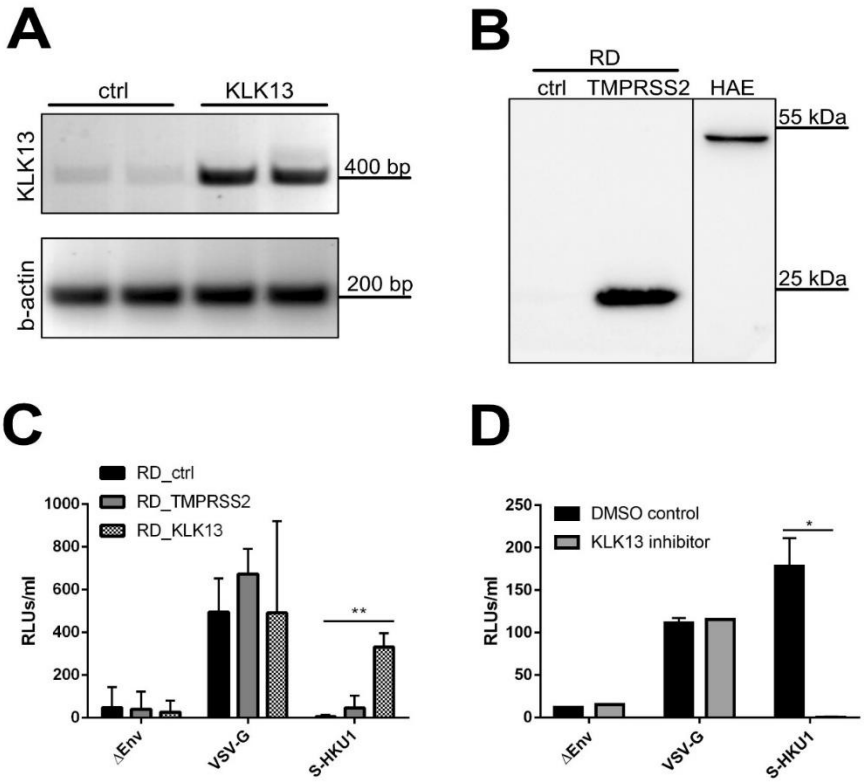

1050

1051 **Figure 4. RD cells expressing KLK13 are permissive for the HCoV-HKU1**
1052 **pseudoviruses.**
1053 (**A**) RD cells were transduced with lentiviral vectors harboring the KLK13 gene (KLK13) or
1054 empty vector (ctrl). The presence of KLK13 mRNA was evaluated in RD cells after blasticidin
1055 selection; β-actin was used as an internal control. (**B**) RD cells were transduced with lentiviral
1056 vectors harboring the TMPRSS2 gene (TMPRSS2) or empty vector (ctrl). After blasticidin
1057 selection, cells were lysed and proteins were analyzed with SDS-PAGE. TMPRSS2 was
1058 detected in RD cell lysates (50 μg of protein per lane) and HAE cultures lysate (25 μg of protein
1059 per lane) using the specific antibody. (**C**) RD control (RD_ctrl), TMPRSS2-expressing
1060 (RD_TMPRSS2) or KLK13-expressing (RD_KLK13) cells were transduced with HIV
1061 pseudoviruses decorated with VSV-G protein (VSV-G), S-HKU1 glycoprotein (S-HKU1) or
1062 control viruses without the fusion protein (ΔEnv). After 72 h at 37°C, the entry of pseudoviruses
1063 was measured by means of luminescence signal in cell lysates. The assay was performed twice,
1064 each time in triplicate, and average values with standard errors are presented. For comparisons
1065 by Student's t-test, **Indicates $P < 0.005$. (**D**) HAE cultures were inoculated with HIV
1066 pseudoviruses harboring VSV-G control protein, S-HKU1 or control viruses without the fusion
1067 protein (ΔEnv) in the presence of KLK13 inhibitor (10 μM) or DMSO. After 72 h at 37°C the
1068 entry of pseudoviruses was measured by means of luminescence signal in cell lysates (RLUs
1069 per ml of lysate sample). The assay was performed in duplicate, and average values with
1070 standard errors are presented. Statistical significance was assessed with the Student's t-test, and
1071 the asterisk indicates $P < 0.05$.

1072 **FIGURE 5.**

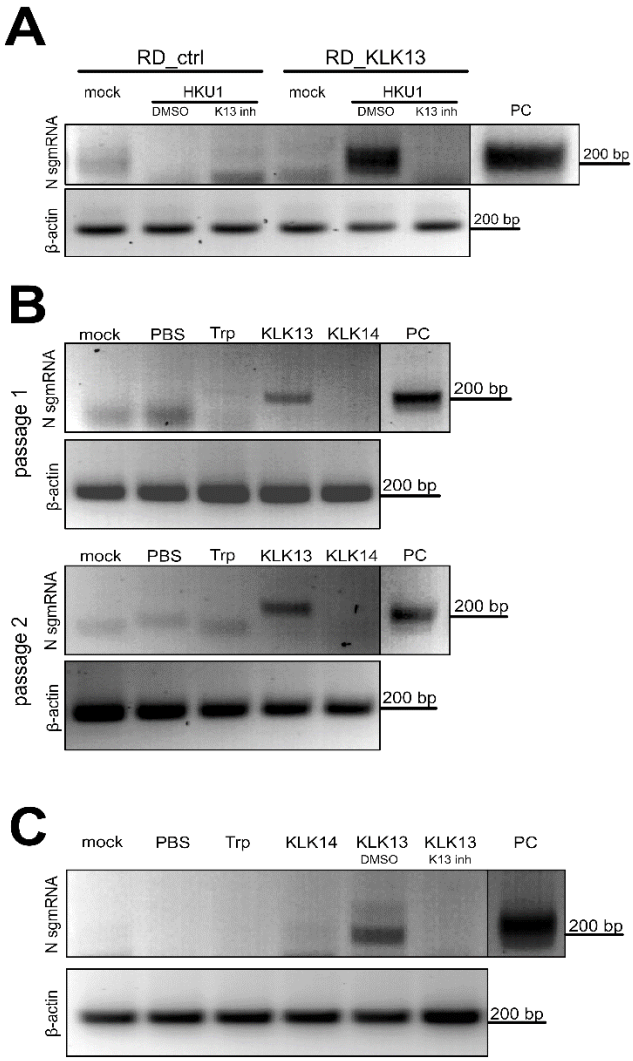

1073

1074 **Figure 5. HCoV-HKU1 replicates in RD cells expressing KLK13 protease.**

1075 (**A**) Control (RD_ctrl) or KLK13-expressing (RD_KLK13) cells were inoculated with HCoV-
1076 HKU1 (10^6 RNA copies per ml) or mock in the presence of 10 μM KLK 13 inhibitor (K13 inh)
1077 or control DMSO. After 7 days culture at 32°C, total RNA was isolated, reverse transcribed and
1078 subgenomic mRNA for N protein was detected in semi-nested PCR, β-actin was used as an
1079 internal control. PC = positive control from virus-infected HAE cells. (**B**) HCoV-HKU1 was
1080 incubated with 200 nM trypsin (Trp), KLK13, KLK14 or PBS for 2 h at 32°C and further
1081 applied on the RD cells. After 7 days at 32°C total RNA was isolated, reverse transcribed and
1082 subgenomic mRNA for N protein was detected in semi-nested PCR (passage 1).
1083 Simultaneously, 1 ml of cell culture supernatant was harvested and applied to freshly seeded
1084 RD cells with medium supplemented with fresh enzymes. After 7 days at 32°C, subgenomic
1085 mRNA for the N protein was detected in semi-nested PCR (passage 2). β-actin was used as an
1086 internal control. (**C**) HCoV-HKU1 was incubated with 200 nM trypsin (Trp), KLK14, KLK13
1087 with KLK13 inhibitor (K13 inh), control DMSO (DMSO), or PBS for 2 h at 32°C and further
1088 applied onto the RD cells. Subgenomic mRNA for N protein was detected in semi-nested PCR;
1089 β-actin was used as an internal control. PC: positive control from virus-infected HAE cultures.

1090 **FIGURE 6.**

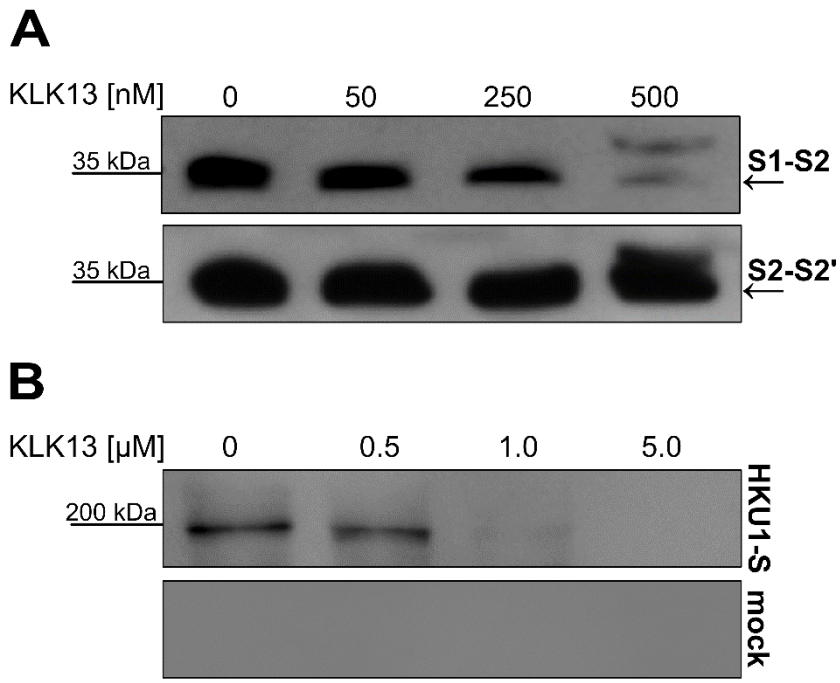

1091

1092 **Figure 6. KLK13 cleaves the HCoV-HKU1 Spike protein between S1 and S2 domains.**
1093 (**A**) 15 ng of CleavEx proteins harboring the S1/S2 or S2/S2' site were incubated at 37ºC for
1094 3 h with different concentrations of the purified KLK13. (**B**) The full-length HKU1-S protein
1095 or mock was incubated at 37ºC for 3 h with different concentrations of the purified KLK13.
1096 After samples denaturation at 95°C, proteins were resolved by SDS-PAGE and detected using
1097 the horseradish peroxidase-labeled anti-His-tag antibody.